# CONCANAVALIN A FUNCTIONALIZED GRAPHENE BASED ELECTROCHEMICAL SENSOR FOR MONITORING CANCER CELLS

**CHAYANIT PHATOOMVIJITWONG**

**A THESIS SUBMITTED IN PARTIAL FULFILLMENT**
**OF THE REQUIREMENTS FOR**
**THE DEGREE OF MASTER OF ENGINEERING**
**(INTEGRATED CHEMICAL ENGINEERING)**
**FACULTY OF GRADUATE STUDIES**
**MAHIDOL UNIVERSITY**
**2017**

Thesis
entitled

**CONCANAVALIN A FUNCTIONALIZED GRAPHENE BASED ELECTROCHEMICAL SENSOR FOR MONITORING CANCER CELLS**

was submitted to the Faculty of Graduate Studies, Mahidol University
for the degree of Master of Engineering (Integrated Chemical Engineering)
on
March 17,2017

.....
Miss Chayanit Phatoomvijitwong
Candidate

.....
Asst. Prof. Piyada Juntawong,
Ph.D. (Genetics, Genomics and Bioinformatics)
Chair

.....
Mr. Sira Srinives,
Ph.D. (Chemical and Environmental Engineering)
Member

.....
Asst. Prof. Theeraporn Rubcumintara,
Ph.D. (Materials Engineering and Science)
Member

.....
Prof. Rachanee Udomsangpetch,
Ph.D. (Immunology)
Member

.....
Prof. Patcharee Lertrit,
M.D., Ph.D. (Biochemistry)
Dean
Faculty of Graduate Studies
Mahidol University

.....
Asst. Prof. Jackrit Suthakorn,
Ph.D. (Biomedical Engineering)
Dean
Faculty of Engineering,
Mahidol University

Thesis
entitled

**CONCANAVALIN A FUNCTIONALIZED GRAPHENE BASED ELECTROCHEMICAL SENSOR FOR MONITORING CANCER CELLS**

.....
Miss Chayanit Phatoomvijitwong
Candidate

.....
Mr. Sira Srinives,
Ph.D. (Chemical and Environmental Engineering)
Major advisor

.....
Prof. Rachanee Udomsangpetch,
Ph.D. (Immunology)
Co-advisor

.....
Prof. Patcharee Lertrit,
M.D., Ph.D. (Biochemistry)
Dean
Faculty of Graduate Studies
Mahidol University

.....
Asst. Prof. Theeraporn Rubcumintara,
Ph.D. (Materials Engineering and Science)
Program Director
Master of Engineering Program in Integrated Chemical Engineering (International program),
Mahidol University

# ACKNOWLEDGEMENTS

This research works have been made possible by the financial support from the annual government grant under Mahidol University. The author would like to extend her sincere gratitude to Dr. Sira Srinives and Prof. Dr. Rachanee Udomsangpetch for their guidance, support and hospitalities throughout the years. The author also thanks Asst. Prof. Dr. Theeraporn Rubcumintara for her kind supports.

Last but not least, the author would like to thanks to Chemical Engineering staffs, Medical Technology staffs, friends from the NANOCEN lab and Chemical Engineering and Medical Technology faculties for their friendship and kind supports.

Chayanit Phatoomvijitwong

CONCANAVALIN A FUNCTIONALIZED GRAPHENE BASED ELECTROCHEMICAL SENSOR FOR MONITORING CANCER CELLS

CHAYANIT PHATOOMVIJITWONG 5837445 EGIC/M

M.Eng. (INTEGRATED CHEMICAL ENGINEERING)

THESIS ADVISORY COMMITTEE: SIRA SRINIVES, Ph.D., RACHANEE UDOMSANGPETCH, Ph.D.

ABSTRACT

Cancer is a cell malfunction disease that leads to morbidity and mortality. Diagnosing of cancer cells and distinguishing cancer from normal cells at an early stage can be greatly beneficial to significantly reducing the lethal rate in cancer patients. Herein, an electrochemical biosensor was fabricated by functionalizing Concanavalin A (Con A), a sugar binding protein on graphene using carbodiimide (EDC) as a zero linker, covalently immobilizing Con A on the graphene structure. The Con A functionalized graphene electrochemical sensor showed good performance in detecting cells and differentiating ovarian cancer cells from normal fibroblast, relying on cells electrochemical activity. The results revealed unique electrochemical patterns of ovarian cancer cells, and good sensitivity of ovarian cancer cells detection in concentration windows of $1x10^4$ to $2x10^7$ cells/ml. The sensor could be of great benefit to early cancer diagnosis, and could be used as a preliminary test that indicates whether the cell is a cancer in a matter of few hours.

KEY WORDS: ELECTROCHEMICAL SENSOR / GRAPHENE / CONCANAVALIN A / OVARIAN CANCER CELLS

56 pages

การศึกษาความต่างศักย์ไฟฟ้าเคมีของเซลล์มะเร็ง โดยใช้เซนเซอร์ไฟฟ้าเคมี
CONCANAVALIN A FUNCTIONALIZED GRAPHENE BASED ELECTROCHEMICAL SENSOR FOR MONITORING CANCER CELLS

ชญานิษฐ์ ปทุมวิจิตรวงศ์ 5837445 EGIC/M

วศ.ม. (วิศวกรรมเคมีบูรณาการ)

คณะกรรมการที่ปรึกษาวิทยานิพนธ์: ศิระ ศรีนิเวศน์ , Ph.D., รัชนีย์ อุดมแสงเพ็ชร, Ph.D.

บทคัดย่อ

มะเร็งเป็นโรคที่เกิดจากความบกพร่อง และผิดปกติในการทำหน้าที่ของเซลล์ โดยเซลล์มะเร็งอาจนำไปสู่ความผิดปกติที่ร้ายแรงของระบบในร่างกาย และอาจเป็นสาเหตุที่ทำให้ผู้เป็นมะเร็งเสียชีวิตได้ ดังนั้นการวินิจฉัย แยกแยะเซลล์มะเร็งในระยะเบื้องต้นได้จะช่วยลดอัตราการเสียชีวิตของผู้ป่วยโรคมะเร็งได้ โดยในงานวิจัยนี้ได้ศึกษาการประกอบอุปกรณ์เซนเซอร์ทางไฟฟ้าเคมีเข้ากับวัสดุร่วมแกรฟีน และโปรตีน Con A (Concanavalin A) โดยใช้สารเคมีเชื่อมพันธะ (EDC) กระตุ้นการสร้างพันธะระหว่างแกรฟีน กับโปรตีน งานวิจัยนี้ได้ใช้เซนเซอร์ทางไฟฟ้าเคมีเพื่อศึกษาการเปลี่ยนแปลงสัญญาณทางไฟฟ้าโดยเปรียบเทียบระหว่างเซลล์มะเร็งรังไข่ และเซลล์ปกติ โดยได้ศึกษาปัจจัยปริมาณของเซลล์มะเร็งรังไข่ และปัจจัยของการผสมเซลล์มะเร็งรังไข่กับเซลล์ปกติ จากงานวิจัยพบว่าเซนเซอร์ทางไฟฟ้าเคมีนี้สามารถแยกความแตกต่างทางสัญญาณไฟฟ้าของเซลล์มะเร็งรังไข่ และเซลล์ปกติได้ เซนเซอร์มีความไวต่อการตรวจวัดสัญญาณทางไฟฟ้าเคมีของปริมาณเซลล์มะเร็งที่ดีที่สุดในช่วงความเข้มข้น $1x10^4$ ถึง $2x10^7$ เซลล์ต่อมิลลิลิตร แต่เนื่องด้วยโปรตีน Con A ไม่ใช่โปรตีนที่จำเพาะเจาะจงต่อเซลล์มะเร็งทำให้ยังต้องมีการพัฒนาเซนเซอร์ต่อไปในอนาคตเพื่อให้เซนเซอร์ทางไฟฟ้าเคมีนี้มีความจำเพาะต่อเซลล์มะเร็งมากขึ้น ทั้งนี้เซนเซอร์ไฟฟ้าเคมีให้ผลลัพธ์ที่รวดเร็ว สามารถแยกแยะระหว่างเซลล์มะเร็งกับเซลล์ปกติได้ และจากการตอบสนองที่ว่องไวของเซนเซอร์ไฟฟ้าเคมีร่วมกับวัสดุแกรฟีนจึงมีประโยชน์อย่างมากในการนำไปใช้วินิจฉัยโรคมะเร็งในเบื้องต้น

56 หน้า

# CONTENTS

# CONTENTS (cont.)

# LIST OF TABLES

# LIST OF FIGURES

# LIST OF FIGURES (cont.)

# LIST OF FIGURES (cont.)

# CHAPTER I
# INTRODUCTION

In Chapter I, research introduction was stated, involving motivation, objectives and scopes of the project.

## 1.1 Motivation

Cancer is one of the most lethal diseases and a leading cause of death in Thailand. Infection, unhealthy life style and wounds can trigger malfunctioning cells to lost their original memories and insanely duplicating themselves. An early and accurate diagnosis are considered the best approach to cope with cancer, significantly enhancing surviving rate of a patient. Cancer is a disease caused by cell dysfunction, cancer cell characteristics are significantly differed from normal cells, including morphology, regeneration, genetic traits, behavior and metabolism [1]. Treatment and diagnosis of cancer are challenging because of cancer cell growth in the invisible part of organs and is ignored by immune system of the body. Since cancer can grow uncontrollably and often spread to surrounding tissue and can metastasis to any part of the body. Cancer cells can release glycoprotein, glycan and nucleic acid, causing excessive presence of these substances on the cellular surface which can be categorized as tumor markers [2]. These biomarkers will have a great impact on cellular surface properties and they can be potentially useful in early cancer diagnosis.

For these reason, Normal and cancer cells can be distinguished by monitoring cellular properties using analytical methods and tools in many ways, e.g. electrochemical potentials from Zeta potential [3], chemical tests from ELISA kits [4], and basic cell staining procedures [5]. All these methods need to be performed by an expertise, are time consuming, and costly. A simple method for cancer cells monitoring is required.

Currently, electrochemical sensor is one popular fields of technology due to a tremendous amount of research works on advanced materials, mainly nanostructures, such as metal/metal oxide nanoparticles, carbon nanotubes and graphene. The nanomaterials can be used to increase the sensitivity of an electrochemical biosensor, leading to greater precision and accuracy. In addition, faster sensor respond could be achieved with nano-sized devices owing to smaller distances [6]. Graphene is a thin layer of carbon nanostructure which has attracted a great deal of attention in recent years due to the unique properties with outstanding charge transfer, mechanical strength, and chemical stability properties. Also graphene structure is enriched of reactive oxygen functional groups, including carboxyl (-COOH) that could be used for enzyme immobilization through covalent binding, such as covalent bond between carboxylic group on graphene and the amino group on protein [7], which make them suitable to be applied to biological sensors. The direct binding between the functional groups of graphene and protein requires linkers, connection molecule, such as 1-Ethyl-3-(3-dimethylaminopropyl) carbodiimide (EDC**)**, activating carboxyl groups leading them to react with amine groups [8].

In this works, the Con A/graphene electrochemical biosensors would be fabricated, and demonstrated for electroactivity differentiation of normal and cancer cells that were observed by cyclic voltammetry electrochemical approach. The advantages in this work approach primarily for direct monitoring of cancer cells, which will be significant in early cancer diagnosis.

## 1.2 Objectives

1.2.1 To study different methods for Con A immobilization on graphene structure, effects of immobilization methods on ovarian cancer cells adhesion.

1.2.2 To study electrochemical activity of ovarian cancer cells and normal fibroblast cells on Con A-functionalized graphene electrochemical sensor

1.2.3 To investigate possibility of introducing graphene-base electrochemical biosensors for a cancer cell monitoring purpose.

## 1.3 Scopes of study

1.3.1 Efficacy of the Con A immobilization methods, Con A physisorption or covalent binding, would be tested by observing number of ovarian cancer cells on ConA/graphene film.

1.3.2 Investigating electrochemical potentials of ovarian cancer cells and normal fibroblast cells using Con A-functionalized graphene electrochemical sensor in a cyclic voltammetry mode.

1.3.3 Variations in cell concentration are $1\times10^4$, $1\times10^5$, $1\times10^6$, $1\times10^7$ and $2x10^7$ cells/ml of ovarian cancer cells and mixed cell solutions consisting of $5\times10^5$ cells/ml of ovarian cancer cells and various concentrations of normal fibroblast cells- $5\times10^5$, $1\times10^6$, $1.5\times10^6$, $2\times10^6$ and $2.5\times10^6$ cells/ml.

# CHAPTER II
# THEORY AND LITERATURE REVIEW

In Chapter II, theory and literature review was stated, involving cancer diagnosis, biosensor detection and electrochemical cell, graphene, concanavalin A and enzyme immobilization on graphene.

## 2.1 Cancer diagnosis

Cancer are mainly resulted from abnormal proliferation of cells in human body. It can start with one malfunctioned cell that spread and survived in suitable conditions. Human normally have certain number of cells for each cell type, due to cellular mechanism that creates "signal" to inhibit cells from unlimited duplications. Problem occurs when the "signal" is missing or incorrectly responded, leading to abnormal cell growth and multiplication that could further develop to tumor. Tumor is a group of cell that spread uncontrollably, which could be benign or malignant. Common skin wart is one example of a benign tumor, occupied limited spaces, close to its original location, and showed no sign of spreading to other area. A malignant tumor, on the other hand, invades surrounding cell tissue and spreads through human body via circulatory or lymphatic systems (metastasis). The malignant tumors are considered harmful cancer that invades and metastasizes other cells, leading to organs malfunction, organ lost or even death. A single altered cell can cause a proliferative cell population (Figure 2.1), progressing to benign adenomas and, then, malignant carcinoma. Next, the cancer cells could penetrate to nearby cells, tissue and, then, blood, gradually extending to human body [9]. It's worth noting here that benign cancer cells can be removed by surgery while malignant tumors could withstand local treatment.

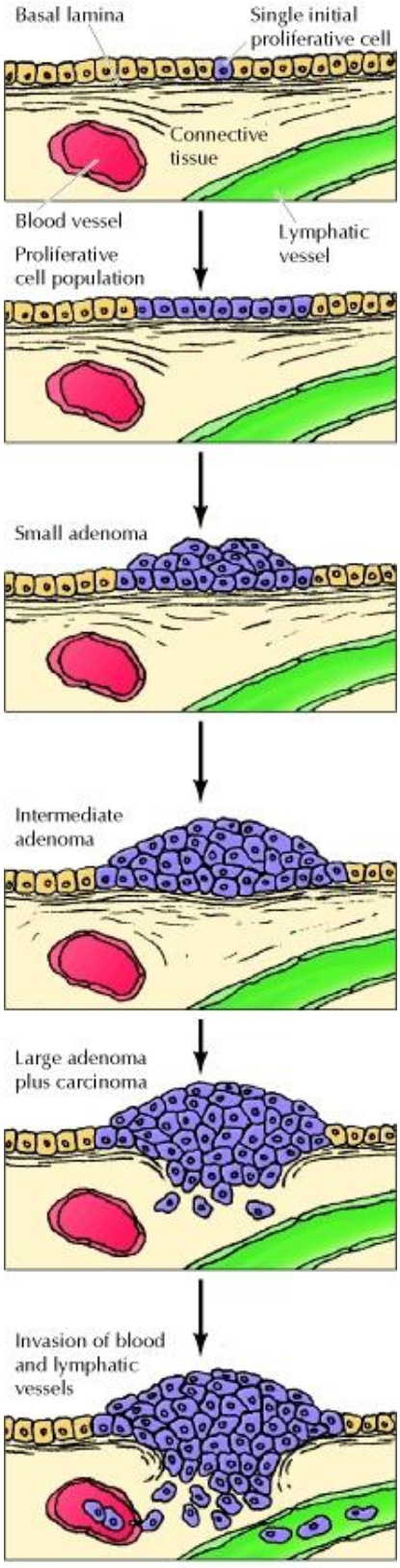


**Figure 2.1 Development of colon carcinomas** [9]

Cancerous cells can be different from noncancerous cells in various aspects. Such changes can occur during cell reproduction and dividing, leading to cell mutation - genetically damage in genes, lost in genetic information, or false replication. Cell mutation can lead to cell "memory lost", an evil step that triggers out of control cell growth that leads to tumors. The mutation of cell to tumors causes changes in cell behaviors, including metabolisms. Cancer cell may release glycoprotein, glycan or nucleic acid causing excessive presence of these substances, which can be indicated as a tumor marker. The marker is potentially useful in screening early cancer diagnosis. For instance, overexpressed glycoproteins on the cellular membrane can influence the properties of the cellular surface. Yi C. et al [10] investigated the expression of c-Kit and platelet-derived growth factor receptor α (PDGFRα), one of the family of receptor tyrosine kinase (RTK) that can be founded in epithelial ovarian tumor cells and stromal tumors. The c-Kit and PDGFRα were involve in cell growth, metastasis, invasiveness and cell proliferation of malignant tumors. In ovarian cancer, the overexpression of these are higher than benign ovarian tumors or normal tissues. In addition, Perfezou M. et al [6] observed that human epidermal growth factor (HER2) is a member of epidermal growth factor receptor (EGFR) tyrosine kinases, which is a glycoprotein, can affect the growth of some cancer cells. The overexpression leads to cancerous cell proliferation and can be founded in a various types of human carcinomas such as lung, breast, and ovarian carcinomas. So far, several diagnosis tests have been used for a diagnosis of cancer cells, such as imaging tests, biopsy and chemical stains and electrochemical techniques.

### 2.1.1 Imaging tests

The basic most technique for a diagnosis of cancer cell is imaging tests, which involves inside human body image capture, locating whereabouts of the suspected cancerous cells. The method can be utilized in several ways:

a) Computerized tomography (CT) Scan

CT scan combines data from X-rays in different angles and transmitted to a computer, producing a 3D-cross section image of structures inside the body and displaying on the screen (figure 2.2). Dye or materials with some forms of label can be applied to specific areas to highlight or provide signals for diagnosis purpose [11].

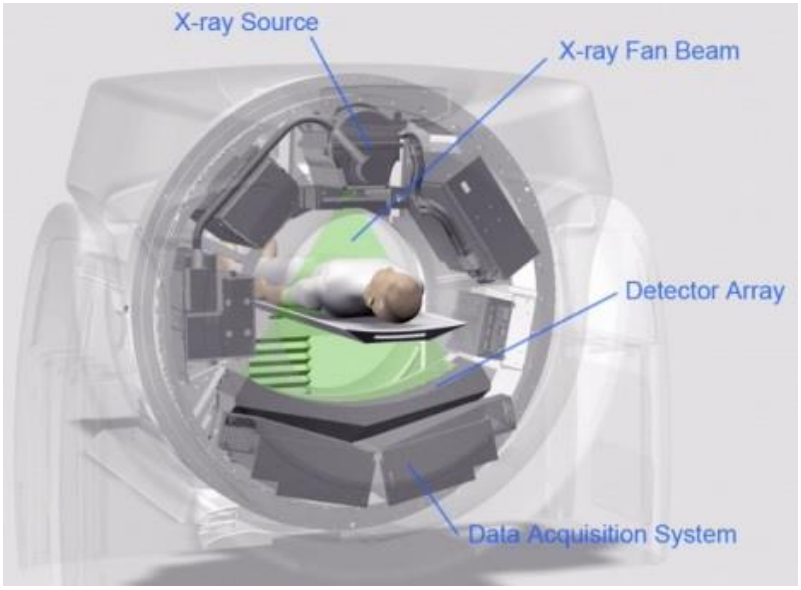


**Figure 2.2 CT scanner** [12]

b) Ultrasound

Ultrasound imaging technique utilizes high frequency sound waves to produce live images of organ inside the body (figure 2.3). The sound waves approach the organs and reflect to a signal-receipting device called transducer. The signals can be used for creation of image, known as sonogram that is displayed on the monitor [13].

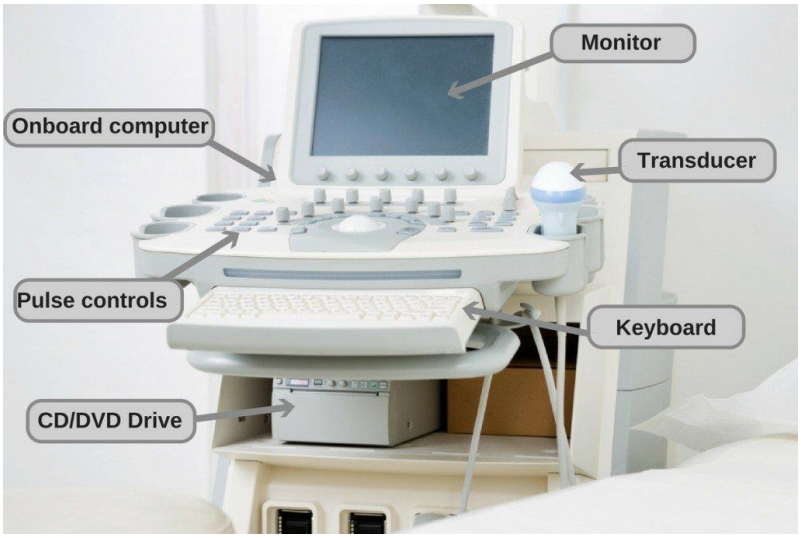


**Figure 2.3 Ultrasound machines** [14]

c) Magnetic resonance imaging (MRI)

MRI technique utilizes a combination of magnetic field and radio waves to generate detailed images of structures and organs inside of the body (figure 2.4). The principle of examination was radio waves handle the magnetic position of nuclei of atoms, which generate rotating magnetic fields and send to a computer. The computer resulting in clearly black and white cross-sectional images inside the body, which can be converted into three-dimensional (3-D) image of the scanned area [15, 16].

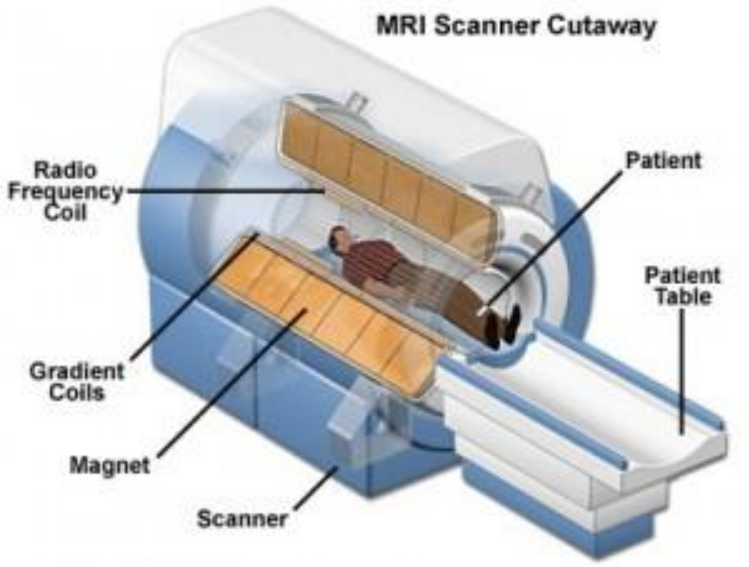


**Figure 2.4 Magnetic resonance imaging scanner** [17]

d) Positron Emission Tomography (PET) scan

PET uses radioactive materials called radiotracers injected into the body and were adsorbed by organs and tissues. The scanner probes that special dyes and produces three-dimensional (3-D) images, showing where the tracer accumulate in the body and showing functionality state of the organs and tissues (figure 2.5) [18].

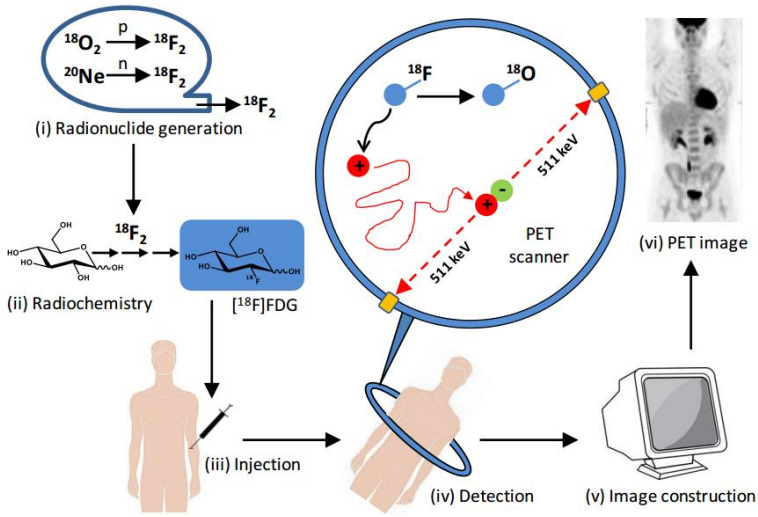


**Figure 2.5 Procedure of PET scan** [19]

These current approaches have been widely used and accepted by doctors, researchers and expertise worldwide. However, they are time consuming, are costly, depend strongly on trained personals, and, unfortunately, contain a considerate level of uncertainty. There are plenty of rooms for improvement as a new approach for cancer diagnosis with high reliability and accuracy with ease of performing is still needed.

### 2.1.2 Biopsy and chemical stains

A biopsy is medical procedure that remove a piece of sample tissue or cell from an organ or body tissue and make it a “specimen”. The specimen can be obtained in several ways, such as punching needle to a defined spot to obtain fluid or tissue sample, using an endoscope, special instrument with a long tube that contains camera and cell acquisition mechanic at the tip, or performing a surgery for tissue sample removal. The tissue would be grinned, dyed and spaded on glass slide prior to an observation under a confocal fluorescence microscope (Figure 2.6) [20, 21].

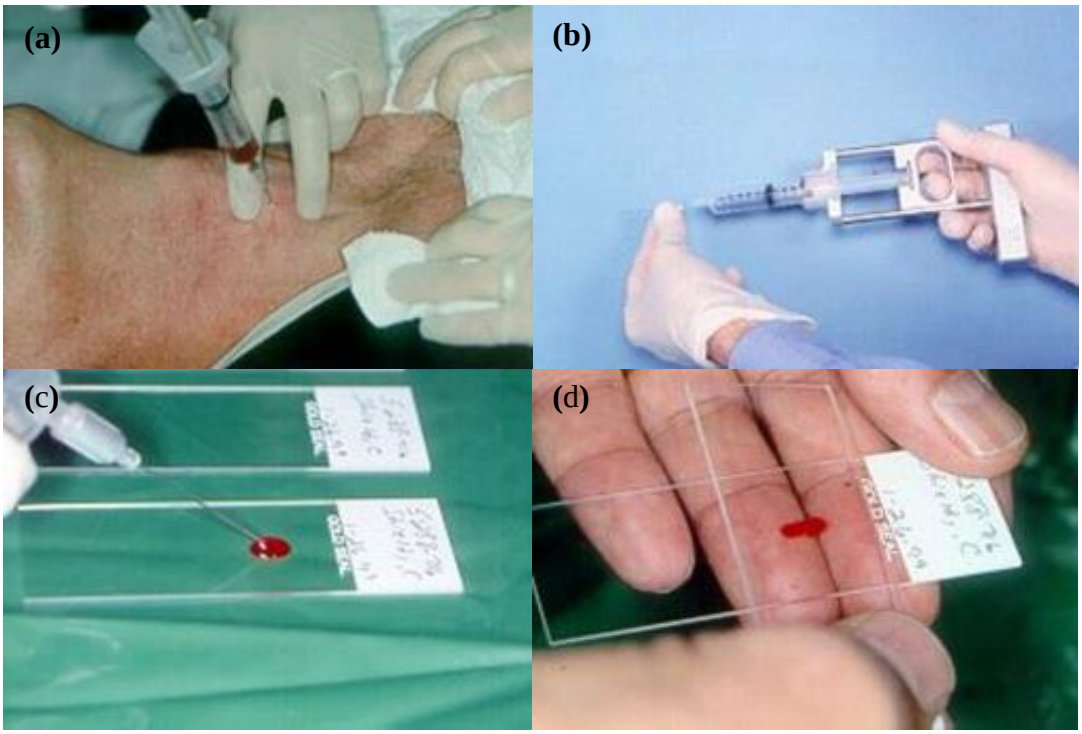


**Figure 2.6 Standard procedures for tissue or cell collection. Collect sampling cell with fine-needle (a), quickly removed needle and aspirated to the syringe (b), dropped sampling on the glass slide (c), and analyzed under a microscope (d)** [22]

There are several approaches, used for attaching tissue specimens on glass slide:

a) Permanent section

The tissue specimen was “fixed” in a formalin solution for several hours. The cell fixation period can be varied depending on specimen’s size and types of cell tissue. The fixation process forces cellular proteins to become fixed and stiff while physical structure of the cell. Then, water is removed from cell tissue, replaced with the paraffin wax. The specimen was cut to an extremely thin slice, floating in the water, and was gently placed on the glass slide. Then, the paraffin was dissolved from the tissue, allowing water to refill the cell structure.

b) Frozen section

To create frozen section, the specimen was quickly frozen after surgery removed, and cut into thin layers with cutting instrument called as cryostat. These specimen placed on glass slide

c) Smear

In this method, the specimen, a liquid or a small pieces of tissue was smeared on the glass slide and let dried in the air. The specimen was further sprayed with fixative solution or submerged in a fixative solution to fix the cell tissue.

The tissue cell can be stained with colored dyes that can be nonspecific or targeting some parts of the cell [23]. Next, the specimen was observed under an optical microscope and characterized in terms of color and size, etc. Although the chemical staining procedure provides extremely accurate results in indicating cancer cells, it involves preparation steps and time consumption, delaying test results by days. Therefore, we are interested in electrochemical detection techniques that can provide real-time monitoring, fast response and reasonable cost.

### 2.1.3 Electrochemical detection techniques

The electrochemical approaches involve monitoring of electrochemical, chemical, electrical, physical properties of an element, attached to the electrode of an electrochemical cell. Cell can also be adhered to the electrode and monitored for electroactivity, relying on changes in biological functionality that affect cell surface properties, or other phenomenon associated with cell membrane. Changes in cell membrane properties could alter charges in cell-electrolyte interface and could be related to cell alteration during cancer transformation.

Cell membranes composes of a bilayer of lipid molecules that act as an electrical insulator, restricting of charged ion mobility from travelling across the membrane. The exchange of intracellular and extracellular charged ions across the cell membrane creates potential difference that provides electrical signals. For a healthy cell, the outer layer of the cell membrane is slightly negatively charged as resulted from various functional groups- amino, carboxyl, and phosphate, including sialic acid molecules on glycolipids and glycoproteins. The groups extended out of the cell membrane, and usually located at terminal position or in the side chain of oligosaccharides. Normal cancer cell would contain even more glycoproteins and more of sialic acid molecules, leading to a highly negative charges on cell membrane as compared to that of a normal proliferating cell [24]. For example, cancer antigen 125 (CA-125) is a glycoprotein antigen that is usually overexpressed by epithelial ovarian

tumours [25], α-Fetoprotein (AFP) is a glycoprotein that associated with hepatocellular carcinoma, and Human epidermal growth factor (HER2) is a glycoprotein that is overexpressed in several malignant tumors, especially breast cancer [26].

In addition, a healthy cell have high concentration of potassium and low concentration of sodium. Ionic concentrations would change drastically once cells are injured or membrane degenerated from carcinogenesis sodium and water flowing in while potassium, magnesium, calcium and zinc going out of the cell. Difference in electrochemical charges, caused by cell functionality, can be monitored electrochemically, and could be used for an indication of carcinogenesis in cells [27].

Recently, electrochemical sensor has been applied to many fields, including cancer monitoring, relying on changes in cell membrane functionality and chemicals produced by cell. For instance, Chen X. et al [28] demonstrated a use of electrochemical sensor for indication of cell carcinogenesis, combining reduced graphene oxide (rGO) with poly(amidoamine) dendrimer (PAMAM) and concanavalin A (Con A). Cells can be immobilized by Con A and further incubated with aptamer-horseradish peroxidase-modified gold nanoparticles (HRP−aptamer−AuNPs) as a nanoprobe (Figure 2.7).

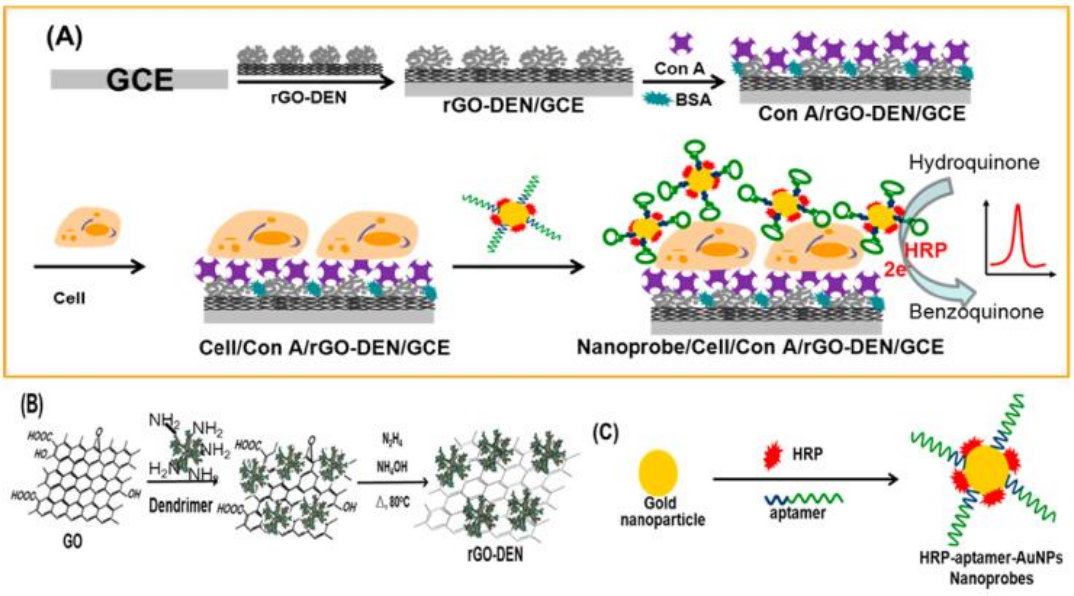


**Figure 2.7 Electrochemical biosensor fabrication (A), PAMAM Dendrimer-Conjugated reduced graphene oxide (rGO−DEN) fabrication (B), and aptamer-horseradish peroxidase-modified gold nanoparticles (HRP−Aptamer−AuNPs) fabrication (C)** [28]

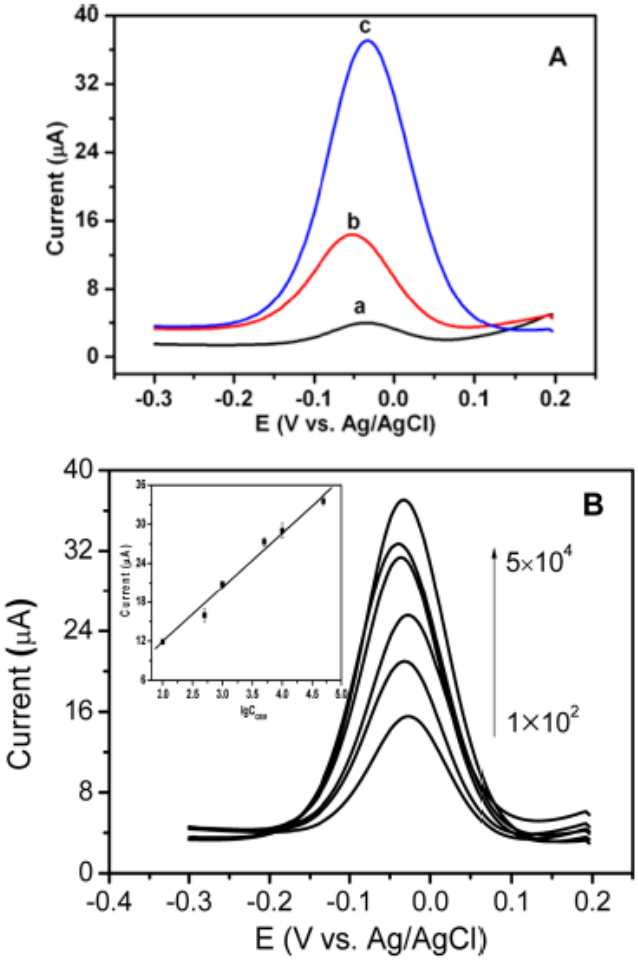


**Figure 2.8 (A) DPV curves of the Con A/rGO−DEN electrode (a), after incubated with HRP−aptamer−AuNP solution (b), and after incubated with CCRF-CEM cells and HRP−aptamer−AuNP solution, respectively (c) and (B) DPV curves of the PAMAM-conjugated rGO-modified electrode incubated with CCRF-CEM cells at various concentrations of $1\times10^2$, $5\times10^2$, $1\times10^3$, $5\times10^3$, $1\times10^4$, and $5\times10^4$ cells/ml** [28]

The signal behaviours of the biosensor (Figure 2.8(A)) was obtained in a differential pulse voltammetry mode (DPV) where peak of Con A/rGO−DEN electrode was observed (curve a). The peak current increased after incubating the electrode with HRP−aptamer−AuNP nanoprobes (curve b), in which HRP is a mannose-containing

glycoprotein with enzymatic activity. The HRP−aptamer−AuNP nanoprobes absorbed on the Con A modified electrode because of the affinity interaction between Con A and mannose groups. When the Con A/rGO−DEN electrode was incubated with human acute lymphoblastic leukemia (CCRF-CEM) cells solution and then incubated with HRP−aptamer−AuNP nanoprobes, the DPV peak current exhibited a sharp peak (c), which was attributed to strong affinity between Con A and mannose groups on the CCRF-CEM cell and highly specific interaction between the aptamer and CCRF-CEM cells. The DPV curves (Figure 2.8(B)) show the sensing signals of the biosensor, incubated with various concentrations of CCRF-CEM cell form $1\times10^2$ to $5\times10^4$ cells/ml. DPV peak currents increased with cell concentrations increased in proportion with the logarithmic value of the cell concentrations with a correlation coefficient (R) of 0.996.

Likewise, Chandra P. et al. [29] demonstrated a use of biosensor, combining gold nanoparticles (AuNPs) with conducting polymer composite and then immobilizing with Permeability glycoprotein (P-gp) antibody (AuNPs/pTTBA/AntiP-gp). Multidrug resistance cancer cells (MDRCC) can be adhered, followed by immobilization of antigen on the surface and then incubated with the aminophenyl boronic acid (APBA) that combining with multi-wall carbon nanotube (MWCNT) to detecting different amount MDRCC and acquired the sensing signal in cyclic voltammogram mode (Figure 2.9).

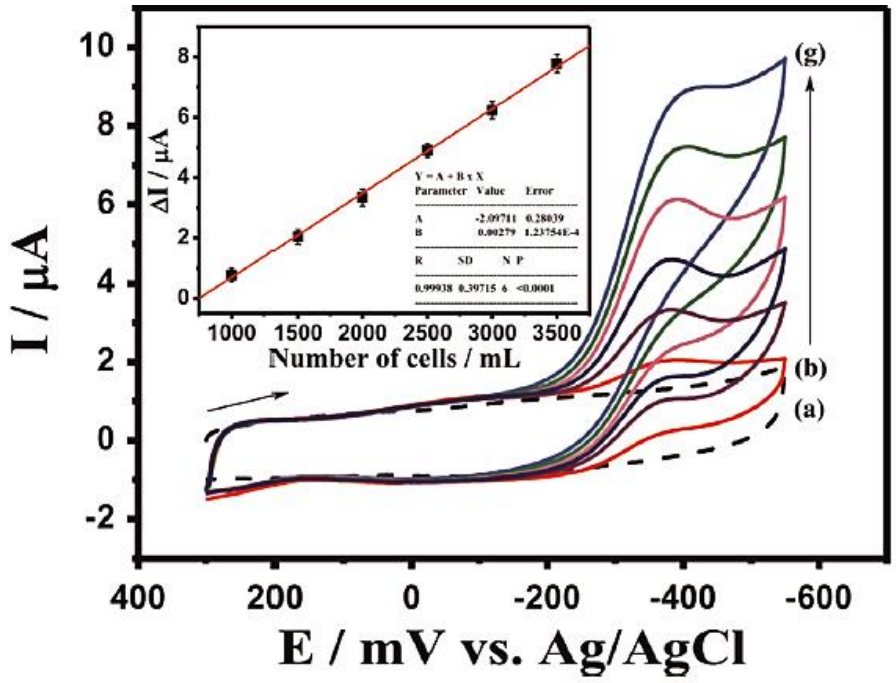


**Figure 2.9 CVs curve of blank background (a), incubated with multidrug resistance cancer cells (MDRCC) cells at different concentrations of 1000, 1500, 2000, 2500, 3000, and 3500 cells/ml (from b to g) using AuNPs/pTTBA/AntiP-gp electrode and Inset shows the calibration curve with increasing of MDRCC** [29]

Their CVs responses (Figure 2.9) increases as the amount of MDRCC increases from 1000 to 3500 cells/ml. The increment in current intensity was in conformation with previous reports, discussed earlier. The Inset (Figure 2.9) shows a linear correlation of response current and cell concentration with a correlation coefficient (R) of 0.997.

## 2.2 Biosensor detection and electrochemical cell

Biosensor is a biomaterial-based sensor that utilizes specificity of biological receptor and efficient charge transfer of semiconductor. Basic mechanisms involve biochemical reactions between biomaterials and target analytes, providing "biological signal" that can be converted by semiconductive sensitive element to "electrical signal".

Biosensor has been developed and applied to various fields of application including blood sugar test, ferment ethanol in beverage, and dissolved oxygen, etc.

### 2.2.1 Electrochemical cell

An electrochemical cell is an electrochemical device that functions as platform for a conversion of electrochemical reactions to electronical signals. It commonly involves 3-eletrode set up; working electrode (WE), reference electrode (RE) and counter electrode (CE) (Figure 2.10).

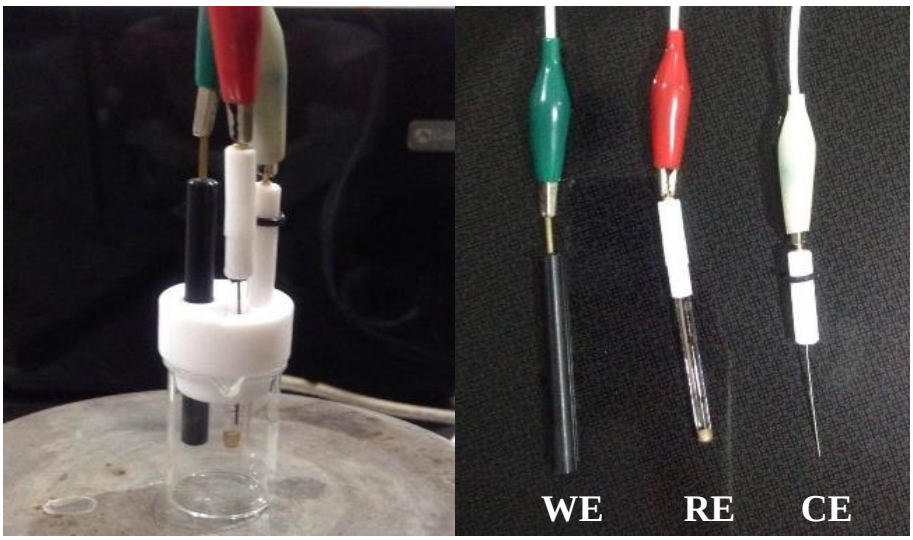


**Figure 2.10 Electrochemical system with three electrodes: working electrode (WE), reference electrode (RE) and counter or auxiliary electrode (CE)**

a) Working electrode (WE) can be glassy carbon, carbon powder, gold, or nickel sheets, and is responsible for redox reaction. Physical/chemical/electrochemical reactions occurred on WE would be monitored and converted to electrical signal.

b) Reference electrode (RE) is the potential reference electrode, in which solution potential is measured and set as "zero". The applied potential provided to WE or CE would be in correspondent to RE. Normal reference electrodes include silver-silver chloride (Ag/AgCl) or standard saturated calomel electrode (Hg/HgCl).

c) Counter or auxiliary electrode (CE) is an addition electrode that is employed to complete the other half of redox reaction. Inert and conducting materials, such as platinum and graphite, are normally used.

In a normal operation, WE would react/interact with target analyte with a motive force from applied potential, monitored with respect to RE, creating electrochemical current. Meanwhile, the other half redox reaction would undergo at CE, completing the redox reaction, and driving electron donation/accepting.

### 2.2.2 Electrochemical techniques

For an electrochemical analysis, various electrochemical signals such as current, potential, charge and impedance can be monitored and recorded via redox reaction, occurred on the working electrode. In a biological analysis, biochemical reactions that involve specific binding, enzymatic reaction, bioreceptor, etc., can be utilized, creating correlation between reaction rate and analyte concentration. One of the most commonly used electrochemical measuring techniques is cyclic voltammetry (CV).

#### Cyclic Voltammetry

Cyclic voltammetry (CV) is one of the most widely used measuring technique in electrochemical analysis, measuring electrochemical current and a function of scanning potential. Cyclic voltammetry is performed by scanning potential, applied to the WE vs. RE, from initial value to a potential edge and scanning potential backward to the other potential edge to complete a scan. Potential scan continues by scanning potential from one potential edge to the other and from the other to the original value (Figure 2.11). While the potential is scanned, electrochemical current passing through WE is recorded [30].

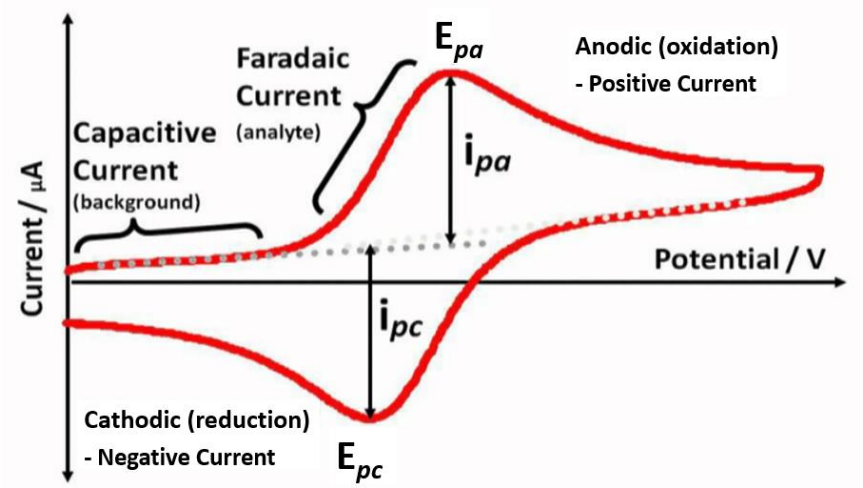


**Figure 2.11 Cyclic voltammogram** [31]

The forward CV scan creates anodic peak (oxidation peak) that correlates to anodic current ($i_{pa}$) while the backward (reverse) scan generates cathodic peak (reduction peak) that correlates to cathodic current ($i_{pc}$). Basic ideas behind the voltamogram phenomenon rely on double layer concept, revolving around electrostatic charge balances on WE. Depending on material used for the WE, functional groups on WE and cell electrolyte cause electrostatic charges at solid-liquid interfaces. Charge polarity on WE is governed by amount of functional groups and their pKa values that dictate total charge polarity at a certain pH. The electrolyte would gradually balance the WE electrostatic charge with radicals with opposite polarity, creating "double charge layers" - an imaginative film consisting of negatively and positively charged layers balancing one another [32]. The double layer acts as electronic capacitor- collecting and releasing charges, depending on applied potential on WE and electrolyte pH. During the initial state, electrical charge transfer on WE involves heavily on charging/discharging of the double layer capacitance. As the potential scans, charging/discharging phenomenon continues and is responsible for hysteresis loop of the CVs. During the potential scan, active radicals from the electrolyte can get involved in redox reaction over the WE, providing anodic peak current ($i_{pa}$) and cathodic peak current ($i_{pc}$), as corresponded to oxidation and reduction reaction, respectively. Peak position and direction indicate anodic and cathodic peak potential ($E_{pa}$ and $E_{pc}$), involving certain radicals

conducting certain reactions. On the other hand, peak intensity can relate to number of charge transfer through the WE that further calibrate to radical concentration in the electrolyte phase. To understand the behavior of the cell under cyclic voltammetry, influences of voltage on the equilibrium established at the electrode surface need to be understood. For example, Cui J. et al. [33] developed a specific technique for cancer cells detection using electrochemical sensor, based on $Au/TiO_2$ nanobelt heterostructure electrodes, and reported results in cyclic voltammogram as shown in figure 2.12.

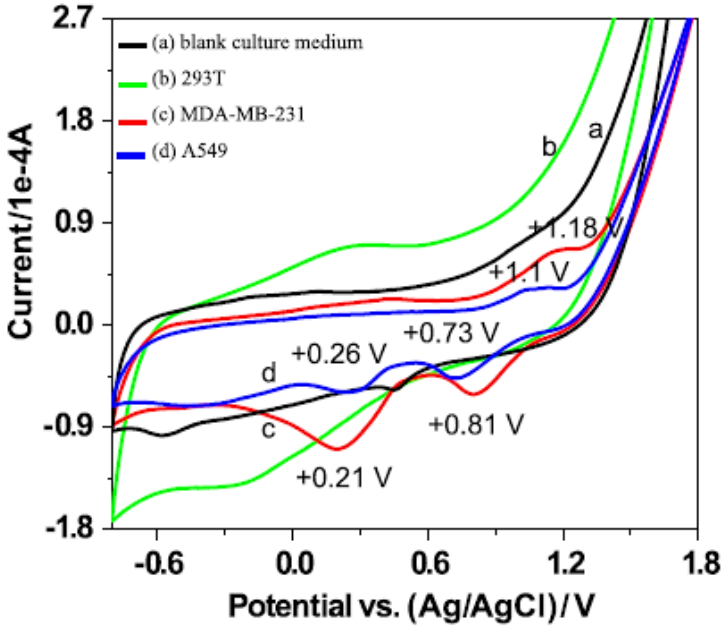


**Figure 2.12 Cyclic voltammograms of blank culture medium (a), the embryonic kidney cells (b), the human breast cancer cells (c) and the human lung cancer cells (d) using the Au/TiO2 nanobelts modified electrode** [33]

The CVs of the normal and cancer cells were different, as shown in Figure 2.12. Normal cells of the embryonic kidney revealed two peaks at -0.25 and 0.3 V. while the human breast cancer cells showed two distinctive peaks on the cathodic side at +0.21 and +0.81 V. Another 2 distinctive peaks were observed from CV of the lung cancer cells (Figure 2.8(d)), one anodic peak at +1.1 V, and two cathodic peaks at +0.26 and +0.73 V. These results show that cancer cells and normal cells exhibit markedly different voltammetric characteristics.

## 2.3 Graphene

Graphene is a two-dimensional (2D) nanostructure of carbon, providing high surface-to-volume ratio, electron transfer rate and thermal stability. These properties offer endless possibilities to highly sensitive detection [34], mechanical reinforcement, and electronic devices. There are 3 main oxidative states for a chemically synthesized graphene, known as graphene, graphene oxide (GO) and reduced graphene oxide (rGO). Graphene is the original form that combines to create a packed graphite layer, consisting of carbon atoms connecting with one another via $SP^2$ hybridization. Each graphene layer weakly interact via $\pi$- $\pi$ interaction that allows graphene sheets to combine and remain as stack. One method to disintegrate graphite to graphene sheets relies on chemical oxidation of oxidizing agent and graphite in strong acid solution. The chemical reactions urge carbon bonds to break and become C-H-O functional groups- carboxyl (COOH), hydroxyl (C-OH), and carbonyl (C=O), etc (Figure 2.13). The functional groups can dissociate depending on PKa value of each group and pH of the solution; however, they remain so negatively charged that lead to repulsion and separation of graphene sheets. Graphene oxide (GO) is produced from oxidized graphene sheets, and since GO contains lots of functional group, it is suffered from low electrical conductivity. Some functional groups can partially be removed from GO by reducing the GO with strong reducing agent, such as hydrazine or ascorbic acid, converting it to reduced graphene oxide (rGO). Based on chemical reduction, oxygen-containing functional groups can be removed from GO, but the broken carbon bonds are not fully fixed. Then, the rGO is rather semiconductor, instead of metallic like the original graphene sheets. The chemical path has been known as chemical exfoliation approach and been one of the most popular method for gram-scale synthesis of graphene [35].

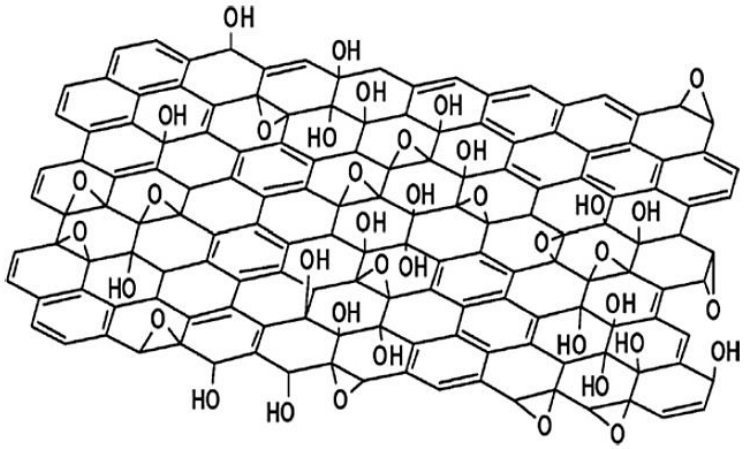

**Figure 2.13 Graphene oxide structure** [36]

## 2.4 Concanavalin A

Concanavalin A (Con A) is a group of plant proteins, known as lectins, which demonstrates an ability to bind with α-D-glucosyl and α-D-mannosyl residues at the non-reducing terminus of oligosaccharides, polysaccharides and cell surface glycoproteins receptor [37]. The affinity of Con A and polysaccharide terminus has been widely applied in cell monitoring such as agglutination, mitogenesis, or cell surface alteration [38]. In order to bind with saccharide sugar, Con A requires a metal ions such as manganese ($Mn^{2+}$) and calcium ($Ca^{2+}$) for the protein transformation. Con A binds with two metal ions per monomer [39, 40], inducing conformation changes of sugar binding site. It is noted that Con A preferentially binds to hydroxyl groups at the C3, C4, and C6 positions of D-glucopyranosyl or D-mannopyranosyl rings, needed in α-glucopyranosides and α-mannopyranosides.

## 2.5 Enzyme immobilization on graphene

Graphene oxide (GO) and reduced graphene oxide are rich in functional groups, which can be utilized for an immobilization of enzyme/protein through covalent binding of "EDC chemistry" [41]. The EDC chemistry relies on chemicals in carbodiimide group, such as 1-ethyl-3-(3-dimethylaminopropyl) carbodiimide (EDC) that reacts specifically with carboxyl group. The EDC-activated carboxyl can further form covalent bond with amino groups from biomolecules prior to a release of EDC from the molecules. GO can firstly be introduced to EDC for an activation of carboxyl group, and exposed later on to the biomolecules for covalent binding [42]. As shown in figure 2.14, Gao Y. et al. [43] reported the covalent coupling of a protein onto CNTs using EDC chemistry.

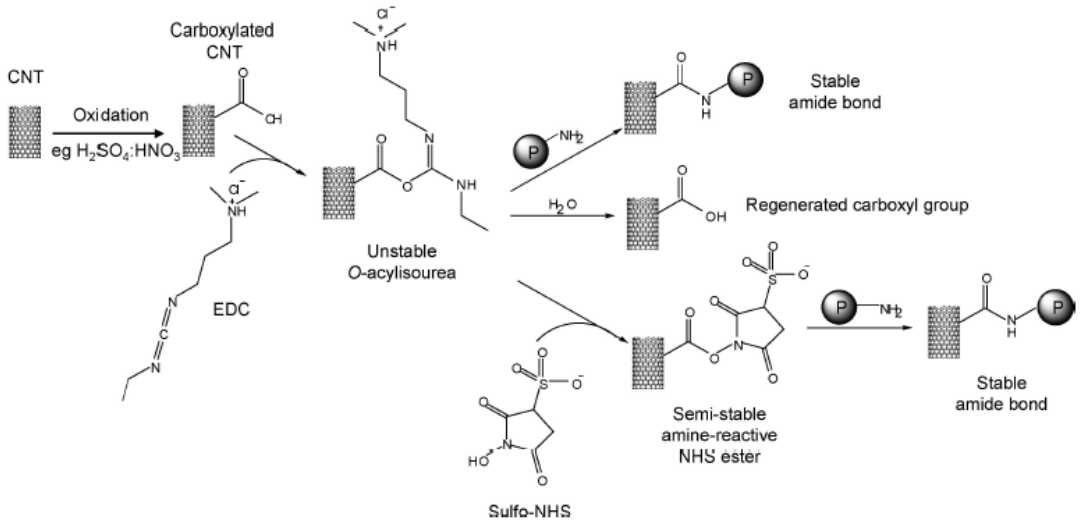


**Figure 2.14 Theoretical mechanism of protein conjugation with EDC to produce carboxylated CNT [43]**

Reaction mechanism of the EDC chemistry is started by a reaction of EDC and carboxyl group that forms an amine-reactive "O-acylisourea" intermediate. The rapid reaction between the intermediate and amino group, form an amide bond and release an isourea by-product (Figure 2.15) [44]. The approach was highly effective and can be applied for the formation of a stable amide bond with a free amine group on proteins.

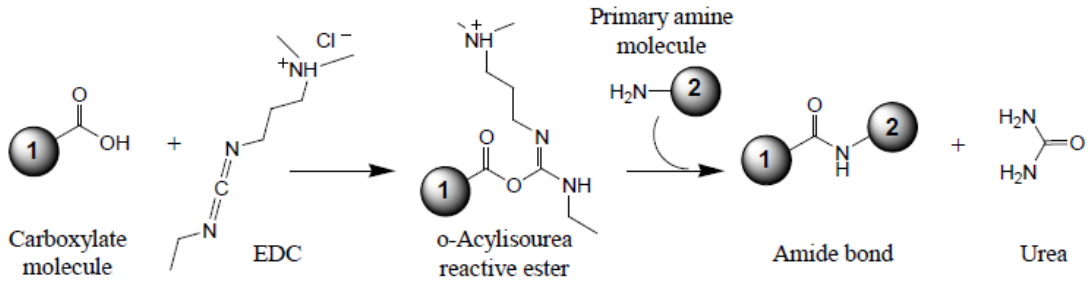


**Figure 2.15 Step of EDC reaction with carboxyl and amino group** [44]

## 2.6 Trypsinization

Trypsinization is the process to dissociate cell by using trypsin, a proteolytic enzyme (hydrolyses proteins) which cleaves peptide chains mainly at the C-terminal side (carboxyl side) of lysine and arginine amino acid residues (Figure 2.16). If the C-terminal side is followed by proline, a type of secondary amine, it could not be hydrolyzed because trypsin can only hydrolyses peptide bond of primary amines [45].

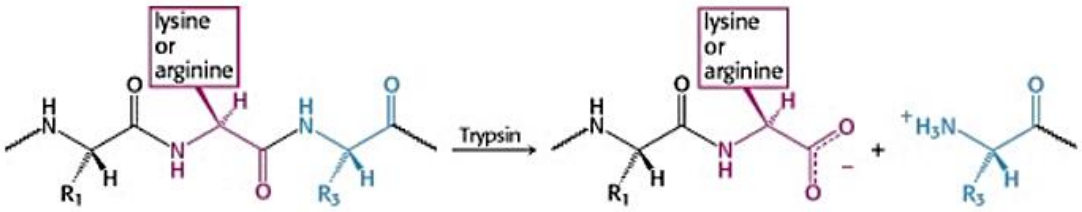


**Figure 2.16 Trypsin hydrolyses peptide bond of arginine and lysine residues** [45]

Trypsinization method is often used to dissociate cell adhesion proteins on the flask in the cell culture and cell-cell interaction that calcium ions is needed. Trypsin usually combines with EDTA, chelator for calcium and manganese ions. Both of these ions inhibit trypsin, causing the concentration of these divalent ions and proteins that could inhibit trypsin to be reduced. However, if cells remain in contact with trypsin for a prolong period, it could cause damage to the protein in cells' membrane. [46].

# CHAPTER III
# RESEARCH METHODOLOGY

The Chapter III concerns materials and method, divided to three section; Materials and methods were including graphene synthesis and cells line preparation, Cell visualization and Electrochemical operations (Figure 3.1).

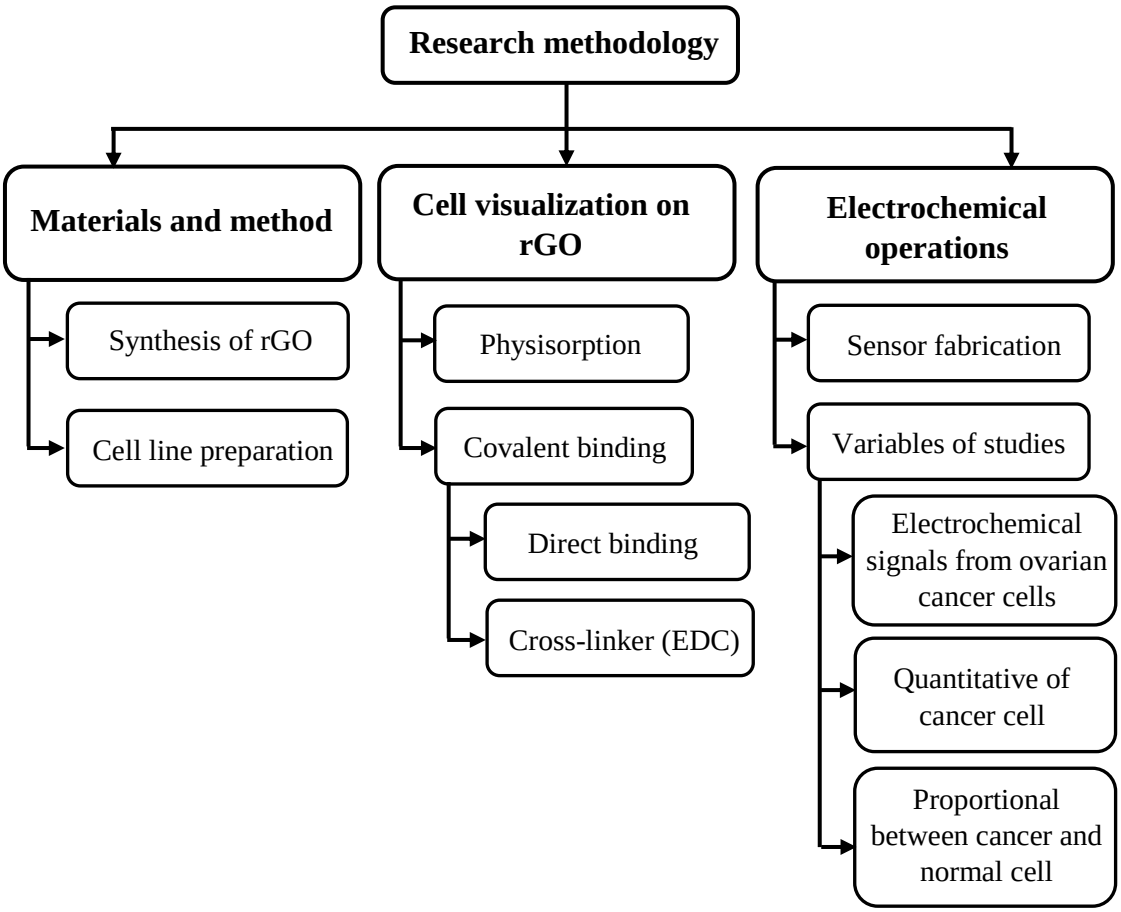


**Figure 3.1 Research methodology plans**

## 3.1 Materials and methods

### 3.1.1 Materials

Graphene oxide (GO) was synthesized from natural graphite flakes (99.9%, -10 mesh, USA) following a modified Hummer's method [35]. All chemicals, including sodium nitrate ($NaNO_3$, 99%), potassium permanganate ($KMnO_4$, Ajax Finechem pty Ltd), hydrogen peroxide (30% $H_2O_2$, Emd millipore corporation), hydrochloric acid (HCl, 37%, V.S.Chem house), sulfuric acid ($H_2SO_4$, 98%, V.S.Chem house), sodium hydroxide (NaOH, 97%, Ajax Finechem pty), MES buffer (4-morpholinoethanesulfonic acid, pH 4.5) were either reagent or analytical grade. Phosphate buffer saline solution (10× PBS, pH 7.4) containing with sodium chloride (NaCl, 137 mM) and potassium chloride (KCl 2.7 mM) was prepared in house. Cell culture medium (RPMI 1640 and DMEM) and Penicillin-Streptomycin were purchased from Gibco (USA). Fetal bovine serum (FBS), trypan blue solution, N-(3-Dimethylaminopropyl)-N’-ethylcarbodiimide hydrochloride (EDC) and Concanavalin A from Canavalia (Jackbean) were purchased from sigma-aldrich. Carboxyfluorescein succinimidyl ester (CFSE) was purchased from BioLegend (USA). All chemicals were analytical grade and used without further treatment.

### 3.1.2 Synthesis of reduced graphene oxide

Synthesis of GO relied on a modified Hummers' method [35] that involved chemical oxidation of graphite with sodium nitrate and potassium permanganate that acts as catalysts in an acid solution to introducing oxygen molecules to the carbon of graphene. The process started by mixing 2 grams of graphite and 1 gram of $NaNO_3$ in a 50 ml concentrated $H_2SO_4$ at 0 ˚C for 2 hrs. During the time, 7.3 g of $KMnO_4$ was added slowly in to prevent the rapid rise of temperature (kept the reaction temperature below 20 ˚C). The mixture was raised to 35 ˚C and stirred for 2 hrs prior to an addition of 90 ml DI water, reducing mixture viscosity. A solution of 7 ml 30% $H_2O_2$ solution and 55 ml water was added in to the mixture to terminate the reaction, yielding brownish color GO powder that can be filtered out using vacuum filtration apparatus. The obtained GO powder was rinsed with 3% HCl and DI water to reduce metal ions before being dried at

90°C for 24 hrs. The GO was thermally reduced at 320°C for 4 hrs, producing reduced graphene oxide (rGO).

### 3.1.3 Cancer and normal cells line preparation

Ovarian cancer cells (A2780) and normal fibroblast cells (L929) were cultured in RPMI 1640 and DMEM medium, respectively. Both cells were supplemented with 10% Fetal bovine serum (FBS) and 1% Penicillin-Streptomycin (10,000 U/ml). Cells were cultured at 37°C with 5% (v/v) $CO_2$ in a humid-saturated atmosphere and were collected using 0.25% trypsin-EDTA. Cells with more than 90% viability, as determined by trypan blue exclusion, were visualized by basic cell staining method using Carboxyfluorescein succinimidyl ester (CFSE). In brief, 1 ml of cell suspension ($10\times10^6$ cells/ml) was mixed with 10 µM CFSE in PBS with 0.1% FBS. The cells were obtained via centrifuge at 2,000 rpm for 5 min, and were rinsed twice in fresh PBS solution. The obtained cells were suspended in medium broth and kept at 4°C for future uses.

## 3.2 Visualization of cell adhesion on rGO

The rGO powder was re-suspended in DI water (2 mg/ml), drop-casted on multiple well glass slides, and dried at 50 °C, creating rGO film layer on the glass slides. For physisoption, rGO-coated glass slide was incubated with well stained ovarian cancer cells for 30 mins, gently rinsed with PBS solution (pH 7.4), and observed under fluorescence microscopy. For covalent binding divided into two methods that are directly binding between the functional groups of graphene and protein and requires linkers (1-Ethyl-3-(3-dimethylaminopropyl) carbodiimide, EDC), the Con A solution for 30 minutes the method are following in figure 3.2.

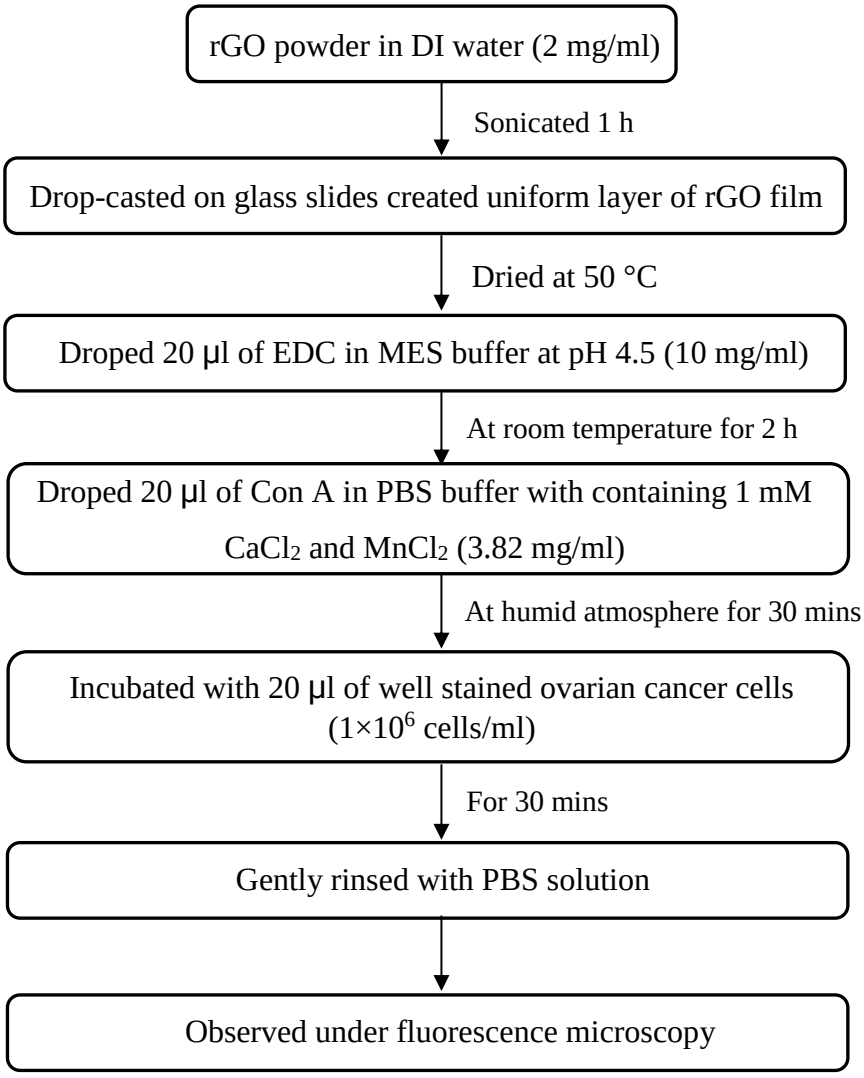


**Figure 3.2 Flow chart of covalent binding method**

## 3.3 Monitoring of electrochemical signal

### 3.3.1 Fabrication of Con A/rGO electrochemical sensor

The rGO powder was re-suspended in DI water (2 mg/ml), drop-casted on a glassy carbon electrode (GCE, diameter of 3 mm), and dried at 50°C, creating the rGO film layer on the GCE. The rGO-coated GCE was introduced to EDC in MES buffer at pH 4.5 (10 mg/ml) for 2 hrs, and immediately exposed to Con A solution with containing

1 mM $CaCl_2$ and $MnCl_2$ (3.82 mg/ml) for 30 mins. The electrode was further exposed to 1% (w/v) BSA in PBS for 30 mins to block nonspecific binding, prior to a gentle rinse with PBS solution.

### 3.3.2 Cancer cell monitoring

**a) Electrochemical signals from ovarian cancer cell**

Ovarian cancer and normal fibroblast cell solution were prepared at $1\times10^6$ cells/ml, dropped (20 µl) on the Con A/rGO electrode, and incubated for 30 mins. The electrode was rinsed with PBS solution (pH 7.4) to remove nonspecific-binding cells. Then, the Cells/Con A/rGO electrode was employed as working electrode (WE) along with platinum wire counter electrode (CE) and reference electrode (RE, Ag/AgCl), electrically connected to CHI1206B electrochemical work station. Electrical potential was applied to the WE. Electrochemical current was monitored and recorded as corresponded to the CV analysis, which was recorded between -0.8 and 1.8 V in 0.1 M PBS solution (pH 7.4).

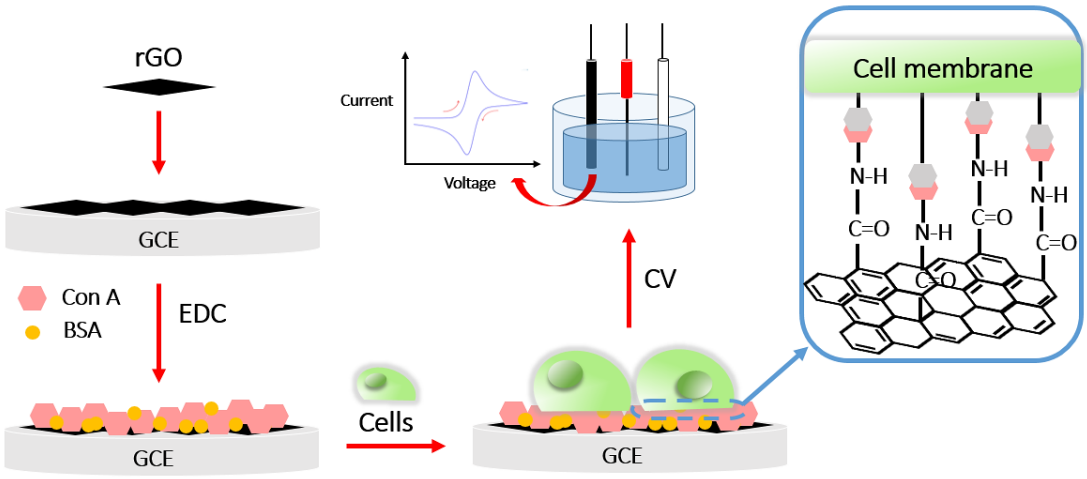


**Figure 3.3 Schematic diagram showing procedures for a fabrication of rGO/Con A electrode and a process for cell monitoring**

**b) Quantitative detection of cancer cells with Con A/rGO electrode**

In this experiment, the Con A/rGO electrode was incubated with different ovarain cancer cell concentrations, varied from $1\times10^4$ cells/ml to $1\times10^5$, $1\times10^6$, $1\times10^7$ and $2x10^7$ cells/ml. Then, drop (20 µl) of a desired concentration of cells on the Con A/rGO electrode, and incubated for 30 mins. The electrode was rinsed with PBS solution (pH 7.4) to remove nonspecific-binding cells. Electrochemical current was monitored and recorded as corresponded to the CV analysis, which was recorded between -0.8 and 1.8 V in 0.1 M PBS solution (pH 7.4).

**c) Mixed solution of cancer and normal cells**

In this experiment, the Con A/rGO electrode was incubated with different ratio of ovarain cancer and normal fibroblast cells. The amount of ovarian cancer cells was fixed at $5\times10^5$ cells/ml while the amount of fibroblast cells was varied from $5\times10^5$ cells/ml to $1\times10^6$, $1.5x10^6$, $2x10^6$ and $2.5x10^6$ cells/ml, respectively. A drop (20 µl) of cell mixture at a desired cell concentration was applied on the Con A/rGO electrode, and let the cells adhered to the electrode for 30 mins (Incubation). The electrode was further rinsed with PBS solution (pH 7.4) to remove nonspecific-binding cells, and was positioned in a electrochemical cell. The electrode was operated in cyclic voltammetry mode whereas electrochemical current was monitored while potential scan of -0.8 to 1.8 V was applied to the electrode. The background solution was 0.1 M PBS solution with a pH value of 7.4.

# CHAPTER IV
# RESULTS & DISCUSSION

## 4.1 Characterizations of GO and rGO

Morphologies of GO and rGO were observed using Scanning electron microscope (SEM) and Transmission electron microscope (TEM) (Figure 4.1). The SEM and TEM images showed geometry of flat sheets with wrinkles of GO (Figure 4.1(a) and (b)) and rGO (Figure 4.1(c) and (d)). Functional groups on GO and rGO were identified on FTIR spectra (Figure 4.2). The FTIR spectra of GO (Figure 4.2(a)) shows the stretching of hydroxyl (-OH) from carboxyl group (-COOH) at 3,400 $cm^{-1}$, the carbonyl stretching (C=O) at 1700-1750 $cm^{-1}$, and the ether or ester groups (C-O) at 1,200 $cm^{-1}$. The FTIR spectra of rGO (Figure 4.2(b)) showed significant reduction at various functional group-related positions. This was attributed to functional group removal during thermal reduction process.

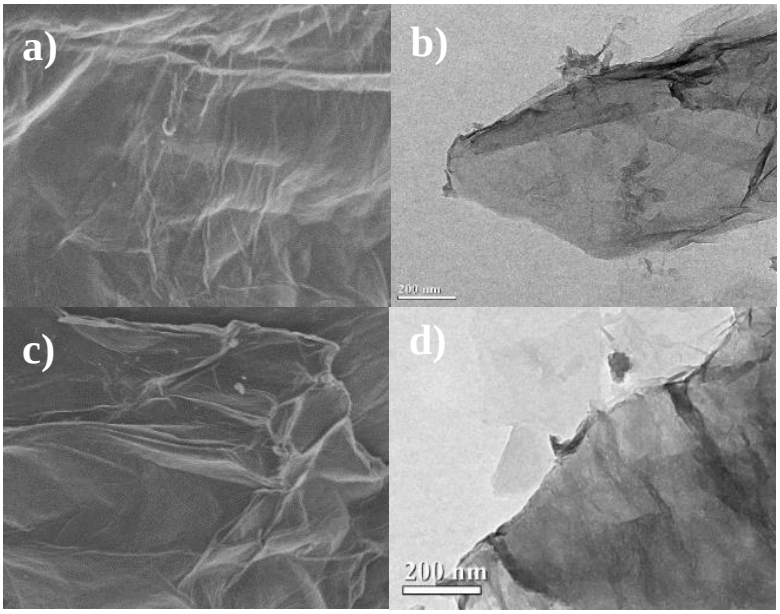


**Figure 4.1 SEM and TEM images showing morphology of GO (a) and (b), and rGO (c) and (d), respectively**

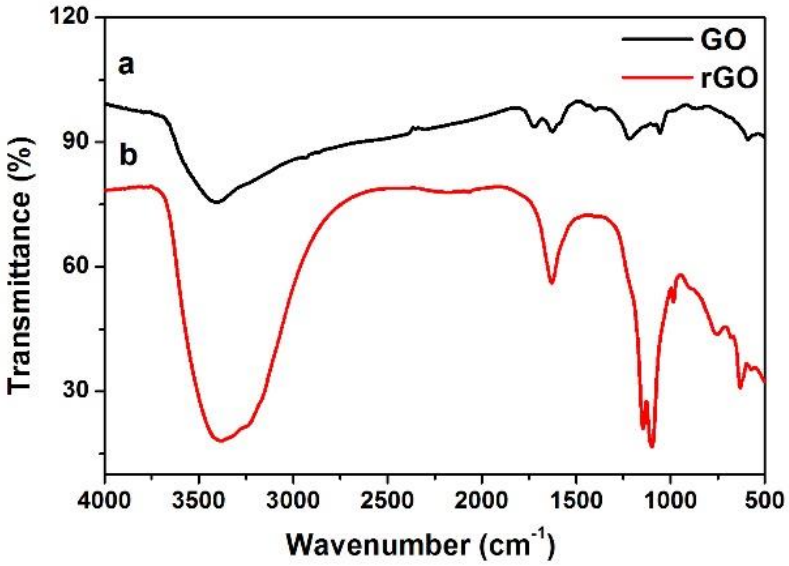


**Figure 4.2 FTIR spectra of rGO (a) and GO (b)**

## 4.2 Visualization of cell adhesion on rGO

For a purpose of visualization, rGO, Con A-physisorbed rGO, and Con A-functionalized rGO were prepared on multiple well glass slides, and incubated with stained ovarian cancer cells ($1\times10^6$ cells/ml) before being rinsed gently with PBS solution. The samples were observed under fluorescence microscopy (Figure 4.3(a-c)). The microscopic images revealed significant effects from rGO modification with Con A, in which the ovarian cancer cells barely adhere to rGO (Figure 4.3(a)), and more cells were observed attached to the Con A/rGO. Technique of Con A immobilization can also play an important effect on cell adhesion since cells were adhered more on the Con A-physisorbed rGO attracted significantly less cells as compared to that of the Con A-functionalized (Figure 4.3(b-c)). This could be attributed to strong binding of Con A to the rGO that yielded convalently-binded Con A a better chance in capturing cells, as compared to the physisorbed Con A. For trypsinization of cell adhesion with the cleavage of peptide bond at the carboxyl side of lysine and arginine amino acid residues seem to not affect the affinity between con A and specific sugar on cellular surface,

which results in cell binding in monolayer and uniformly distributed on graphene (Figure 4.3(b-c))

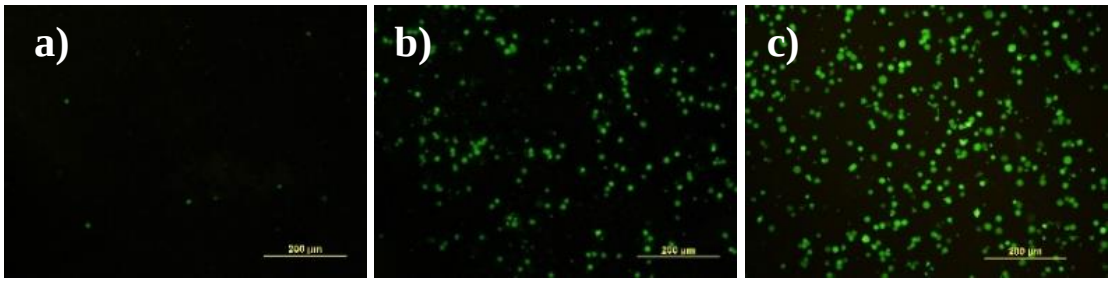


**Figure 4.3 Fluorescence microscopy images of the ovarian cancer cells (A2780) on rGO (a), Con A/rGO (Physisorption) (b) and Con A/rGO (EDC) (c)**

## 4.3 Electrochemical signals from ovarian cancer cells

Electrochemical activity of the cells on working electrode were investigated using cyclic voltammetry (CV) in 0.1 M PBS buffer and the voltage window of -0.8 V to 1.8 V (50 mV/s scan rate). The CV analysis on rGO, Con A/rGO, ovarian cancer cells/Con A/rGO (Incubated with $1\times10^6$ cells/ml) and Fibroblast cells/Con A/rGO (Incubated with $1\times10^6$ cells/ml) revealed voltammograms, shown in Figure 4.4. The voltammogram from rGO electrode was set as an initial background (Figure 4.4(a)), showing an anodic peak at +0.75 V and strong cathodic peak at +0.51 V. The whole voltammogram was flattered after functionalized with Con A on rGO (Con A/rGO, Figure 4.4(b)), indicating charge transfer blockage due to passivation effect from Con A protein [44]. It was observed that fibroblast cells provided no significant response to the Con A/rGO electrode (Figure 4.4(c)). However, one cathodic peaks at +0.63 and one anodic peak at +1.16 V were distinctively indicated from ovarian cancer cells (Ovarian cancer cells/Con A/rGO, Figure 4.4(d)). The electrochemical activity that was obtained from ovarian cancer cells was distinguishable from background current and hypothetically an exclusive cellular property (Figure 4.4(d) Inset). The observed electrochemical signals could be attributed to unique characteristic of the ovarian cancer

cells that might involve electrochemical activity of cell wall components [33, 47, 48]. Two possible factors for electrochemical signal generation are redox reactions that involve

- Functional groups on cell wall, such as glycoprotein, glycan or nucleic acid that often overexpressed on cancer cells surface [49, 50] and/or
- Metabolized chemicals released from the cell.

Redox peaks from cells-laden electrode were observed (Figure 4.4(d)) and compared with the electrochemical signals from Con A/rGO electrode (Figure 4.4(b)), with no cell. Unique signal patterns were observed from the ovarian cancer cells, as resulted from two possible factors that were previously mentioned.

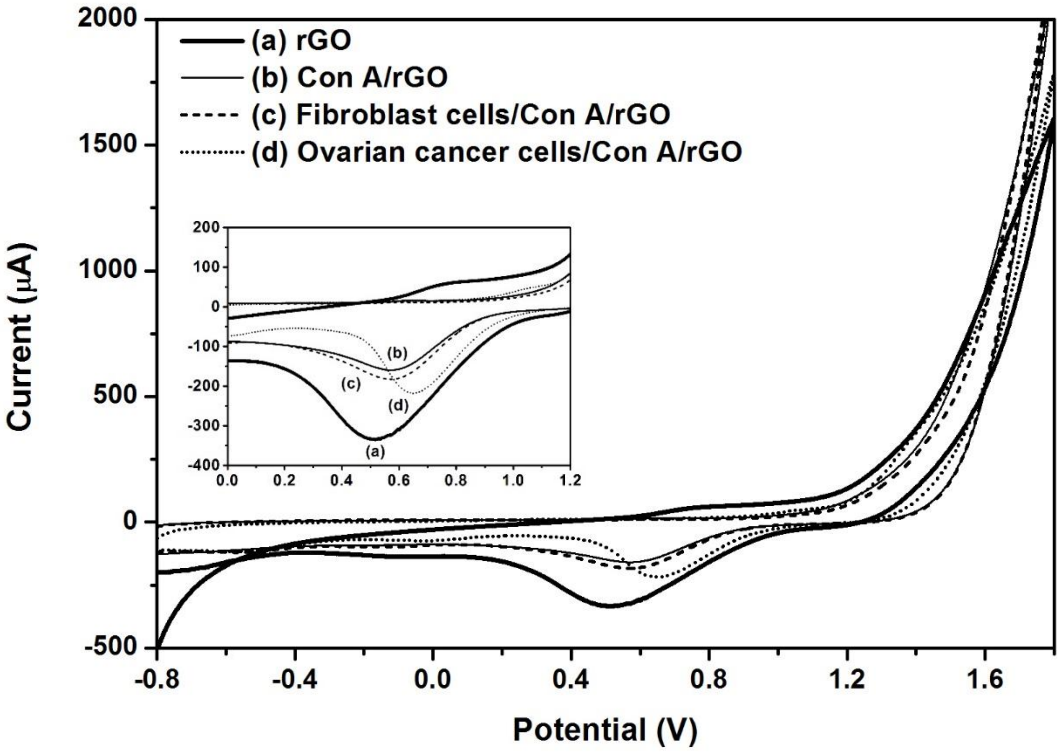


**Figure 4.4 Cyclic voltammograms of rGO (a), Con A/rGO (b), Fibroblast cells/Con A/rGO (c) and Ovarian cancer cells/Con A/rGO (d) in 0.1 PBS buffer (pH 7.4)**

## 4.4 Quantitative detection of cancer cells with Con A/rGO electrode

The highly sensitive device for cancer cells detection can be crucial in an early stage cancer diagnosis. The Con A/rGO electrode was incubated with different ovarian cancer cell concentrations, varied from $1\times10^4$ cells/ml to $1\times10^5$, $1\times10^6$, $1\times10^7$ and $2x10^7$ cells/ml, respectively. The cyclic voltammograms (Figure 4.5) showed good correlation of electrochemical current and cell concentration since the current intensity increased as the ovarian cancer cell concentration increased. Cathodic current from the cathodic peak at +0.63 V was determined from each voltammogram and plotted against logarithmic scale of ovarian cancer cell concentrations (Figure 4.6). Linear correlation between cathodic currents and logarithamic of ovarian cancer cell concentrations was observed with regression equation of

$$Y = -103.88X + 167.42 \qquad \text{(equation 3.1)}$$

where Y was the cathodic current and X was the logarithmic of ovarian cancer cell concentrations and has a correlation coefficient of 0.9411.

These results showed good electrochemical responses from the ovarian cancer cells of the Con A/rGO sensor can be further investigated and developed to basic principle for cancer cell diagnosis.

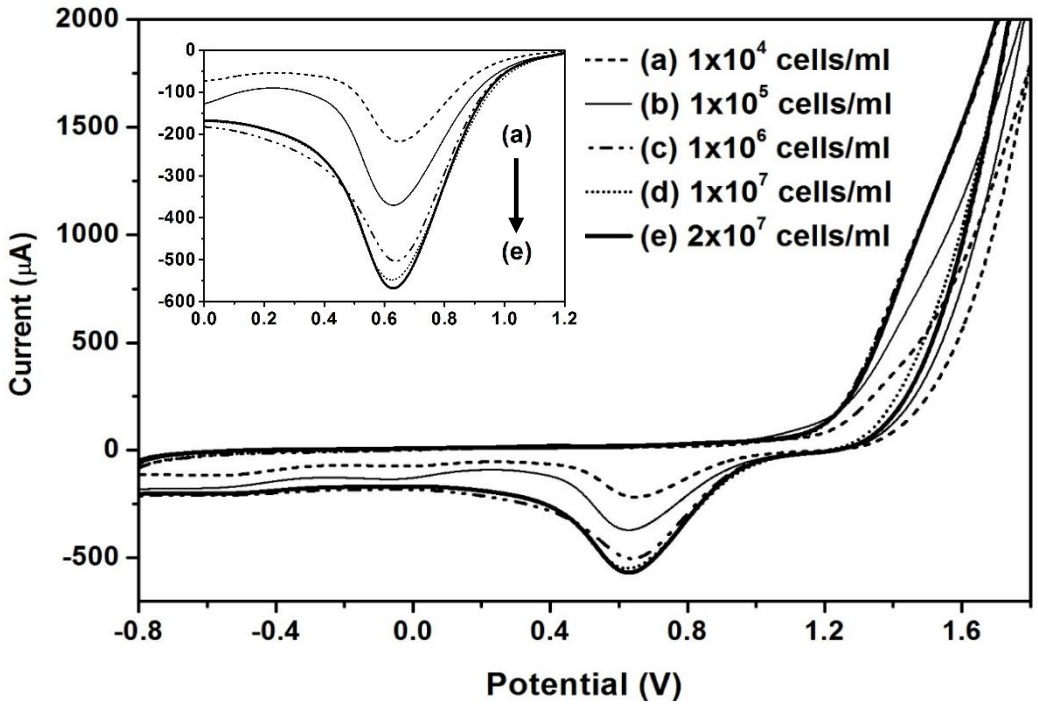


**Figure 4.5 Cyclic voltammograms of Con A/rGO electrode, corresponded to different ovarian cancer cell concentrations from $1\times10^4$ to $2\times10^7$ cells/ml (from a to e)**

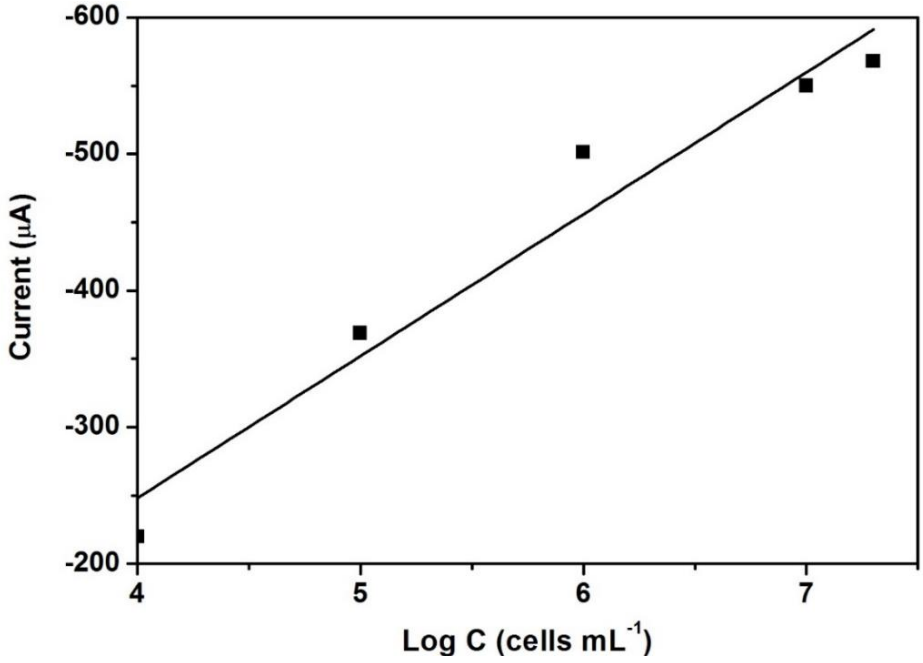


**Figure 4.6 Correlation of electrochemical currents and logarithmic values of ovarian cancer cells concentration**

## 4.5 Interference from normal cells to cancer cells

Although it was clear that Con A was not a very selective protein, and would not provide much specificity to cancer cells, it is worth investigating if there is any preference in term of normal and cancer cells capturing performance. In this case, normal fibroblast cells were used as interences to cancer cells, in which the Con A/rGO electrode was incubated with solutions of cell mixture. The solution consisted of $5\times10^5$ cells/ml of ovarian cancer cells mixed with normal fibroblast cells at various concentrations of $5\times10^5$, $1\times10^6$, $1.5\times10^6$, $2\times10^6$ and $2.5\times10^6$ cells/ml. The Con A/rGO electrode was incubated with a desired cell solution for 30 mins, and further rinsed with 0.1 M PBS buffer 3 times to remove nonspecific binding cells. The electrode was employed in the electrochemical cell and analyzed in the cyclic voltammetry mode. The results, shown in Figure 4.7, revealed that cyclic voltametry curves presenting only unique electrochemical characteristics of ovarian cancer cells with no distinctive signals from the normal fibroblast cells in the tested concentration window. However, the normal fibroblast cells interference occurred as the cathodic currents from the ovarian cancer cells were clearly lowered with a denser amount of the fibroblast cells (figure 4.8). This could be attributed to competitive binding effects between the fibroblast cells and cancer cells since Con A was not a specific protein.

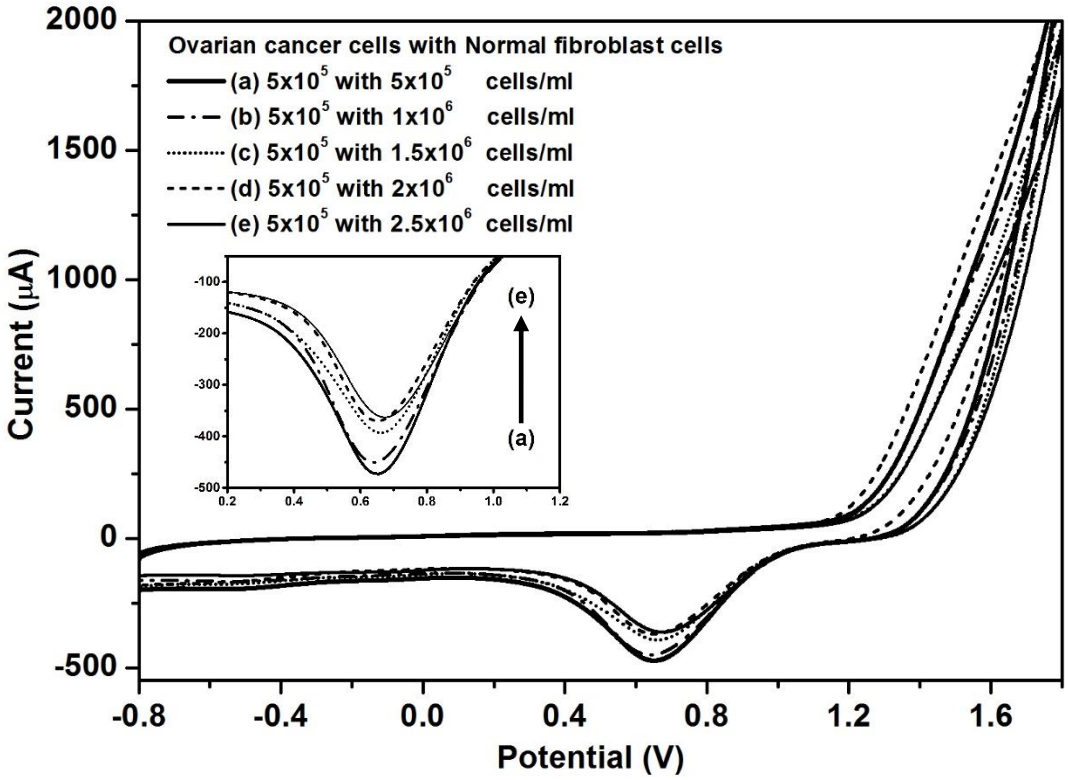


**Figure 4.7 Cyclic voltammograms of Con A/rGO, corresponded to different proportional concentration between $5\times10^5$ cells/ml of ovarian cancer cells with various concentrations of normal fibroblast cells from $5\times10^5$ to $2.5\times10^6$ cells/ml (from a to e)**

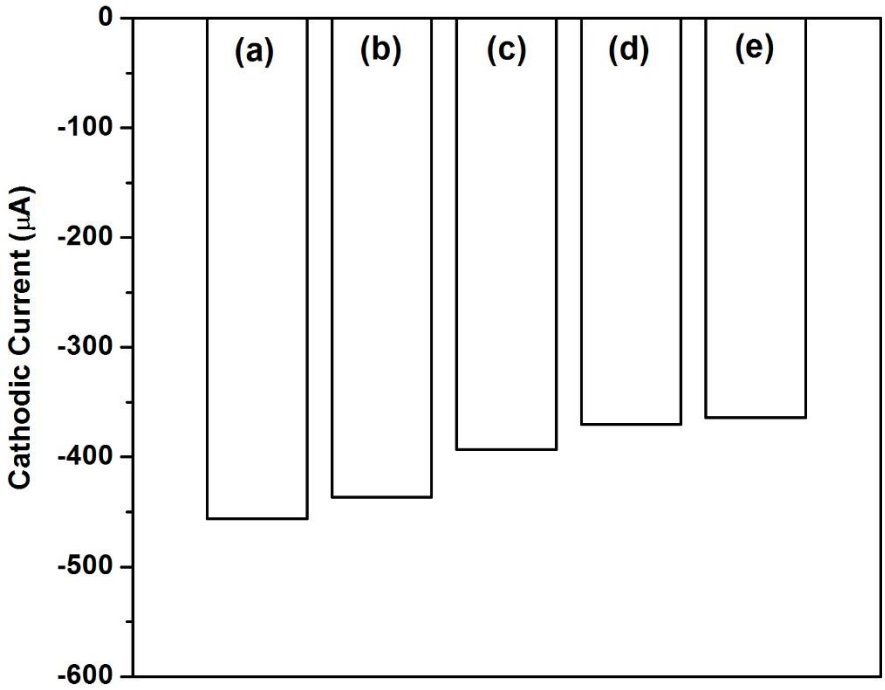


**Figure 4.8 Cathodic current, corresponded to different proportional concentration between $5\times10^5$ cells/ml of ovarian cancer cells with various concentrations of normal fibroblast cells from $5\times10^5$ to $2.5\times10^6$ cells/ml (from a to e)**

After all, the Con A/rGO electrochemical sensor offers a prominent approach for cancer monitoring as it can differentiate ovarian cancer cell from normal fibroblast cell, relying on electrochemical characteristics of cells. In a process of cell biopsy for cancer diagnosis, the obtained cells specimen, instead of being smeared on glass slide and observed under optical microscope for cell appearances, can be applied on the Con A/rGO electrode and characterized for the electrochemical activities. This could help reducing the amount of time required in cancer diagnosis, or could serve as a test for pre-diagnosis. Comparison of the electrochemical method and others (Table 4.1) revealed advantages of the method that can lead to a great advancement in cancer diagnosis.

**Table 4.1 Comparison of methods to diagnosis of cancer**

| Method | Real-time monitoring | Trained personals | Cost | Time |
|---|---|---|---|---|
| CT Scan [12] | No | Needed | High | Time-consuming |
| Ultrasound [14] | Yes | Needed | High | Time-consuming |
| MRI [17] | No | Needed | High | Time-consuming |
| Electrochemical sensor | Yes | No needed | Low | Rapid |

# CHAPTER V
# CONCLUSION

This research demonstrated uses of Con A-graphene materials as a transducer for a detection of cancer cells. The Con A protein was covalently immobilized on the rGO substrate via EDC chemistry, and was visualized to provide good results in capturing ovarian cancer cells. The Con A/rGO electrochemical sensor were successfully prepared and demonstrated for a detection of ovarian cancer cells in cyclic voltammetry mode. The sensor can differentiate normal cell from cancer cell by monitoring their electroactivity, and revealed unique electrochemical pattern for ovarian cancer cells. Good performances of the electrochemical sensor can be attributed to high charge transfer ability of graphene. The Con A/rGO sensor showed high sensitivity and a rapid response to ovarian cancer cell concentrations between $1\times10^4$ to $2\times10^7$ cells/ml. Nevertheless, Con A was not a very selective protein, and would not provide much specificity to cancer cells. The electrochemical sensor could be of great benefit to early cancer diagnosis, in which it can be used as a preliminary test that indicates whether the cell if a cancer in a matter of few hours.

## Suggestion

Future research in this direction is emphasize toward the design, and implementation of more specific that can be better for monitoring cancer cells. For instance, using antibody or substances that specific for types of cancer.

# REFERENCES

1 Cantor, J.R., Sabatini, D.M. (2012). Cancer cell Metabolism: One Hallmark, Many Faces. Cancer discovery, 1-18.

2 Esteller, M., Cespedes, M.S., Rosell, R., Sidransky, D., Baylin, S.B., Herman, J.G. (1999). Detection of Aberrant Promoter Hypermethylation of Tumor Suppressor Genes in Serum DNA from Non-Small Cell Lung Cancer Patients. CANCER RESEARCH, 59, 67-70.

3 Dobrzyńska, I., Skrzydlewska, E., Figaszewski, Z.A. (2013). Changes in Electric Properties of Human Breast Cancer Cells. J membrane Biol, 246, 161-6.

4 Erdile, L.F., Smith, D., Berd, D. (2001). Whole cell ELISA for detection of tumor antigen expression in tumor samples. Journal of Immunological Methods, 258, 47-53.

5 Guinee, D.G., Fiahback, N. F., Koss, M.N., Abbondanzo, S.L., Travis, W.D. (1994). Anatomic Pathology, 102, 406-13.

6 Perfezou, M., Turner, A., Merkoçi, A. (2012). Cancer detection using nanoparticle-based sensors. Chemistry Society Reviews, 41, 2606-22.

7 Zhang, Y., Wu, C., Guo, S., Zhang, J. (2013). Interactions of graphene and graphene oxide with proteins and peptides. Nanotechnol, 2(1), 27-45.

8 Reza, K.K., Ali M., Srivastava, S., Agrawal, V.V., Biradar, A.M. (2015). Tyrosinase conjugated reduced graphene oxide based biointerface for bisphenol A sensor. Biosensors and Bioelectronics, 74, 644-51.

9 Cooper G.M. A Molecular Approach, second edition. Sunderland: Boston University Press 2000

10 Yi, C., Li, L., Chen, K., Lin, S. and Liu, X. (2012). Expression of c-Kit and PDGFRα in epithelial ovarian tumors and tumor stroma. Oncology Letters, 3, 369-72.

11 Christian Nordqvist [serial online] 2017 Jan 26. Available from: http://www.medicalnewstoday.com/articles/153201.php. Accessed Dec 23, 2016.

12 Test and Measurement World [serial online]. Available from: http://www.test-and-measurement-world.com/Equipments/Biomedical/CT-scan-machine-vs-MRI-scan-machine-vs-Ultrasound-scan-machine-types.html. Accessed Dec 24, 2016.

13 Cancer.Net Editorial Board [serial online] 2016 Feb. Available from: http://www.cancer.net/navigating-cancer-care/diagnosing-cancer/tests-and-procedures/ultrasound. Accessed Dec 23, 2016.

14 Science ABC [serial online] 2016 Aug. Available from: https://www.scienceabc.com/innovation/how-ultrasound-scanning-sonography-3d-sonogram-work-pregnancy-due-date.html. Accessed Dec 23, 2016.

15 WebMD [serial online]. Available from: http://www.webmd.com/a-to-z-guides/magnetic-resonance-imaging-mri#1. Accessed Dec 23, 2016.

16 Tanya Lewis [serial online] 2014 Dec 5. Available from: http://www.livescience.com/39074-what-is-an-mri.html. Accessed Dec 23, 2016.

17 Pancreatic cancer action [serial online] 2015 Aug 4. Available from: https://pancreaticcanceraction.org/about-pancreaticcancer/diagnosis/second-line-investigations/mri-scan/. Accessed Dec 24, 2016.

18 Milton Guiberteau [serial online] 2017 Jan 23. Available from: http://www.radiologyinfo.org/en/info.cfm?pg=pet. Accessed Jan 25, 2017.

19 Simon G. Patching (2015). Roles of facilitative glucose transporter GLUT1 in [$^{18}$F] FDG positron emission tomography (PET) imaging of human diseases. Journal of Diagnostic Imaging in Therapy, 2(1): 30-102.

20 Cancer.Net Editorial Board [serial online] 2015 Apr. Available from: http://www.cancer.net/navigating-cancer-care/diagnosing-cancer/reports-and-results/after-biopsy-making-diagnosis. Accessed Jan 30, 2017.

21 American Cancer Society [serial online] 2015 Jul 30. Available from: https://old.cancer.org/acs/groups/cid/documents/webcontent/003185-pdf.pdf. Accessed Jan 30, 2017.

22 Dean, D., Gharib, H. [serial online] 2015 Apr 26. Available from: https://www.ncbi.nlm.nih.gov/books/NBK285544/. Accessed Jan 30, 2017.

23 American Cancer Society [serial online]. Available from: https://www.cancer.org/treatment/understanding-your-diagnosis/tests/testing-biopsy-and-cytology-specimens-for-cancer/special-tests.html. Accessed Jan 30, 2017.

24 Narayanan, S. (1994). Sialic Acid as a Tumor Marker. ANNALS OF CLINICAL AND LABORATORY SCIENCE, 24(4), 376-84.

25 Huang, J., Hu, W., Sood, A. (2010). Prognostic Biomarkers in Ovarian Cancer. Cancer Biomark, 8(0): 231–51.

26 Stowell, S., Ju, T., Cummings, R. (2015). Protein Glycosylation in Cancer. Annu Rev Pathol, 10, 473–510.

27 Haltiwanger, S. [serial online] 2015 Apr 26. Available from: https://www.royalrife.com/haltiwanger1.pdf. Accessed Feb 5, 2017.

28 Chen, X., Wang, Y., Zhang Y., Chen, Z., Liu Y., Li, Z., et al. (2014). Sensitive Electrochemical Aptamer Biosensor for Dynamic Cell Surface N‑Glycan Evaluation Featuring Multivalent Recognition and Signal Amplification on a Dendrimer−Graphene Electrode Interface. Anal. Chem., 86, 4278-86.

29 Chandra, P., Noh, H.B., Pallela, R., Shim Y. (2015). Ultrasensitive detection of drug resistant cancer cells in biological matrixes using an amperometric nanobiosensor. Biosensors and Bioelectronics, 70, 418-25.

30 Rezai, S. (2003). Electrochemical cell and electrodes for cyclic voltammetry. Chem, 174.

31 Das, S. (2013). Cyclic Voltammetry. Urrjaa.

32 Concept of double layers [serial online]. Available from: https://sites.google.com/a/g.clemson.edu/ionic-liquids/home/concept-of-double-layers. Accessed Feb 11, 2017.

33 Cui, J., Chen, J., Chen, S., Gao, L., Xu, P., Li, H. (2016). Au/$TiO_2$ nanobelt heterostructures for the detection of cancer cells and anticancer drug activity by potential sensing. Nanotechnology, 27, 1-8.

35 Razieh, S., Mohsen, J., Ali, R., Ali, G. (2013). Synthesis and Characterization of Thermally-Reduced Graphene. Iranica Journal of Energy & Environment, 4(1), 53-9.

36 Pei, S., Cheng, H.M. (2011). The reduction of graphene oxide. Carbon, 50(9), 3210–28.

37 Sigma Aldrich [serial online]. Available from: http://www.sigmaaldrich.com/content/dam/sigmaaldrich/docs/Sigma/Datasheet/c0412dat.pdf. Accessed Dec 20, 2016.

38 Becker, J., Reeke, G., Wang, J., Cunningham, B., and Edelman, G. (1975). The Covalent and Three-Dimensional Structure of Concanavalin A. III. Structure of the Monomer and its Interaction with Metals and Saccharides. J Biol Chem, 250(4), 1513-24.

39 Grimaldi, J., and Sykes, B. (1975). Concanavalin A: A Stopped Flow Nuclear Magnetic Resonance Study of Conformational Changes Induced by $Mn^{2+}$, $Ca^{2+}$, and alpha-Methyl-D-Mannoside. J Biol Chem, 250(5), 1618-24.

40 Magnuson, J., Alter, G., Appel, D., Chistie, D., Munske, G., Pandolfino, E. (1983). Metal ion binding to concanavalin A. Biosci., 5, 9–17.

41 Pavlidis, I.V., Patila, M., Bornscheuer, U.T., Gournis, D., Stamatis, H. (2014). Graphene-based nanobiocatalytic systems: recent advances and future prospects. Trends in Biotechnology, 32(6), 312-20.

42 Grabarek, Z., Gergely, J. (1990). Zero-length crosslinking procedure with the use of active esters. Anal Biochem, 185, 131-5.

43 Gao, Y., Kyratzis, I. (2008). Covalent Immobilization of Proteins on Carbon Nanotubes Using the Cross-Linker 1-Ethyl-3-(3-dimethylaminopropyl) carbodiimide—a Critical Assessment. Bioconjugate Chem., 19(10), 1945-50.

44 ThermoFisher scientific [serial online]. Available from: https://www.thermofisher.com/th/en/home/life-science/protein-biology/protein-biology-learning-center/protein-biology-resource-library/pierce-protein-methods/carbodiimide-crosslinker-chemistry.html Accessed Sep 9, 2016.

45 Berg J.M., Tymoczko J.L., Stryer L. Biochemistry, Fifth edition. New York: W.H. Freeman Press 2002.

46 Huang, H., Hsing, H., Lai, T., Chen, Y., Lee, T., Chan, H. et al. (2010). Trypsin-induced proteome alteration during cell subculture in mammalian cells. Journal of Biomedical Science, 1-10.

47 Petelska1, B., Dobrzyńska, I., Sulkowski, S., Figaszewski, Z. (2012). Characterization of the Cell Membrane During Cancer Transformation. Colorectal Cancer Biology-From Genes to Tomor, Dr. Rajunor Ettarh (Ed.), InTech, Available from: http://www.intechopen.com/books/colorectal-cancer-biology-from-genes-to tumor/characterization-of-the-cellmembrane-during-cancer-transformation. Accessed Dec 25, 2016.

48 Nakayama, K., Nakayama, N., Katagiri, H., Miyazaki, K. (2012). Mechanisms of Ovarian Cancer Metastasis: Biochemical Pathways. International Journal of Molecular Sciences, 13, 11705-11717.

49 Patankar, M., Gubbels, J., Felder, M., Connor, J. (2015). The immunomodulating roles of glycoproteins in epithelial ovarian cancer. Front Biosci, 4, 631-650.

50 Chatterjee, M., Mohapatra, S., Ionan, A., Bawa, G., Fehmi, R., Wang, X. (2006). Diagnostic Markers of Ovarian Cancer by High-Throughput Antigen Cloning and Detection on Arrays. Cancer Res, 66(2), 1181–90.

# APPENDICES

# APPENDIX A

## Preparation of visualization of cell adhesion on rGO

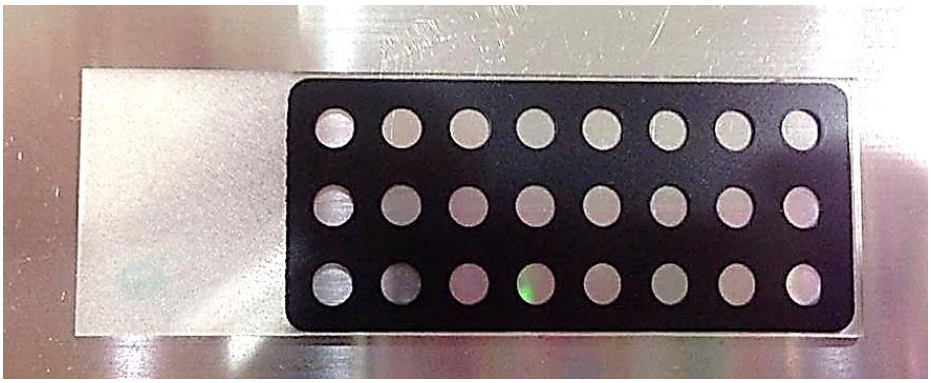

**Figure A.1 Preparation of multiple well glass slides by treated with ethanol solution**

**Figure A.2 rGO powder was re-suspended in DI water (2 mg/ml)**

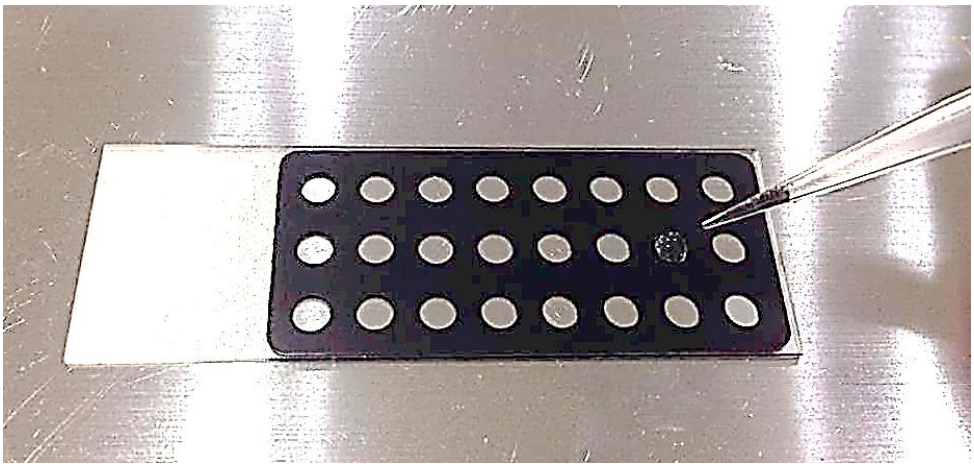

**Figure A.3 Drop-casted rGO suspended on multiple well glass slides**

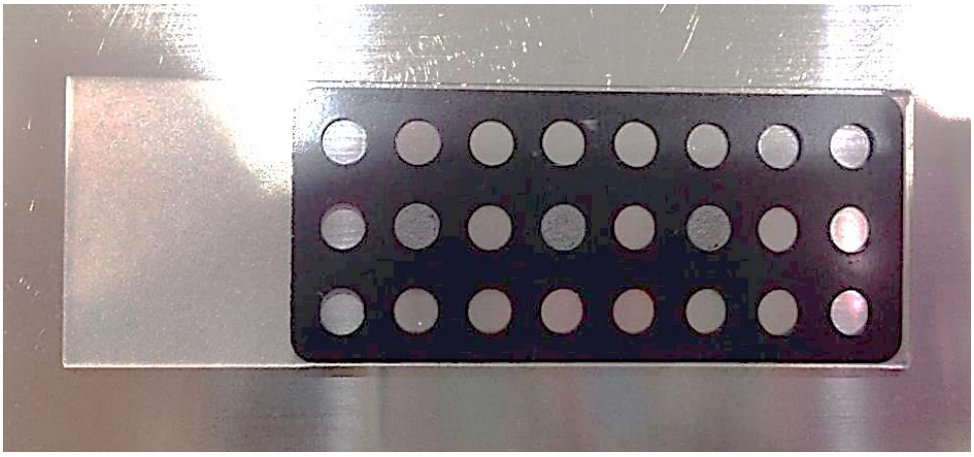

**Figure A.4 Dried at 50 °C, creating rGO film layer on the glass slides**

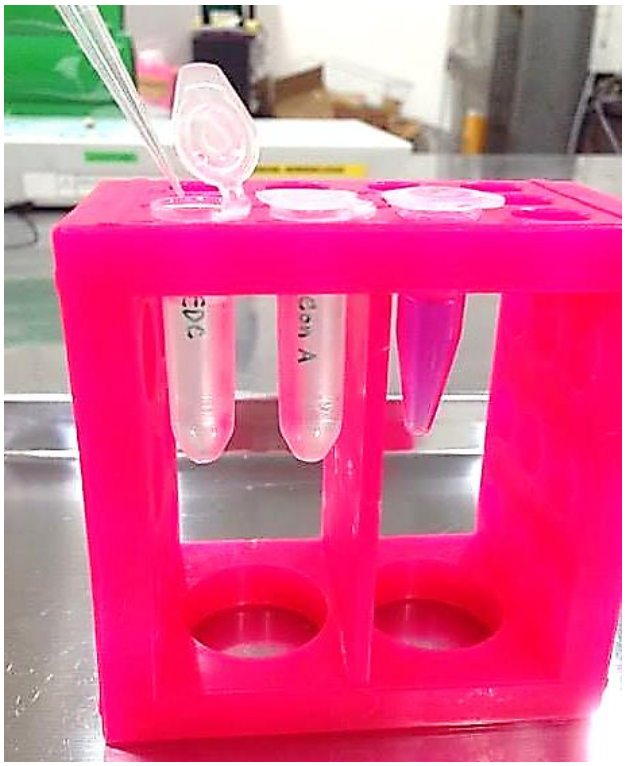


**Figure A.5 Droped 20 µl of EDC in MES buffer at pH 4.5 (10 mg/ml) after 2 hrs, droped 20 µl of Con A in PBS buffer with containing 1 mM $CaCl_2$ and $MnCl_2$ (3.82 mg/ml) for 30 mins, and then incubated with 20 µl of well stained ovarian cancer cells ($1\times10^6$ cells/ml) for 30 mins**

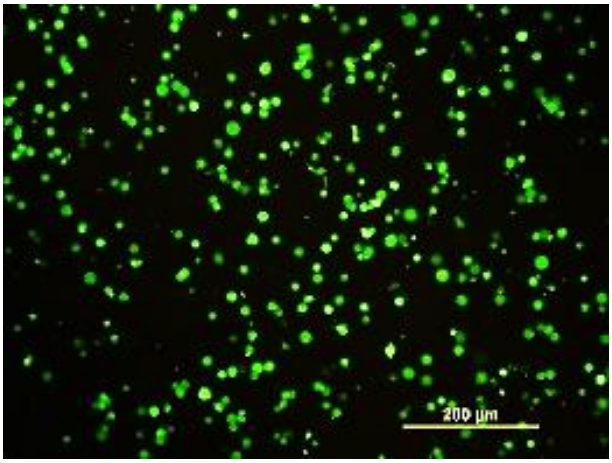


**Figure A.6 Image of well stained ovarian cancer cells observed under fluorencence microscopy**

# APPENDIX B

## Preparation of ovarian cancer cells on electrochemical sensor

**Figure B.1 rGO powder was re-suspended in DI water (2 mg/ml)**

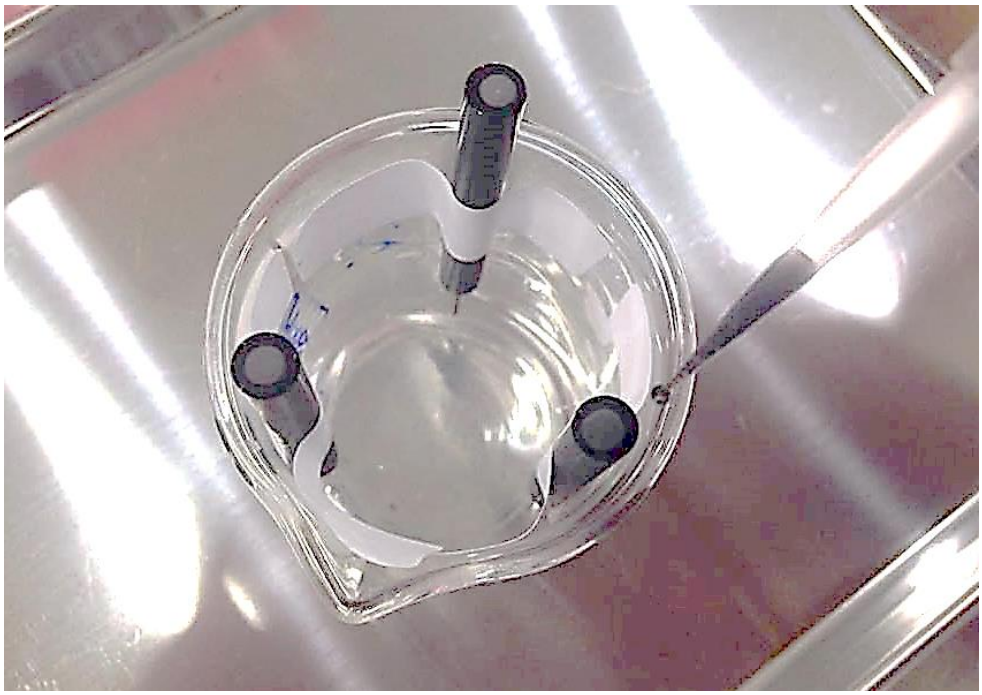

**Figure B.2 Drop-casted rGO suspended on the electrode sensor**

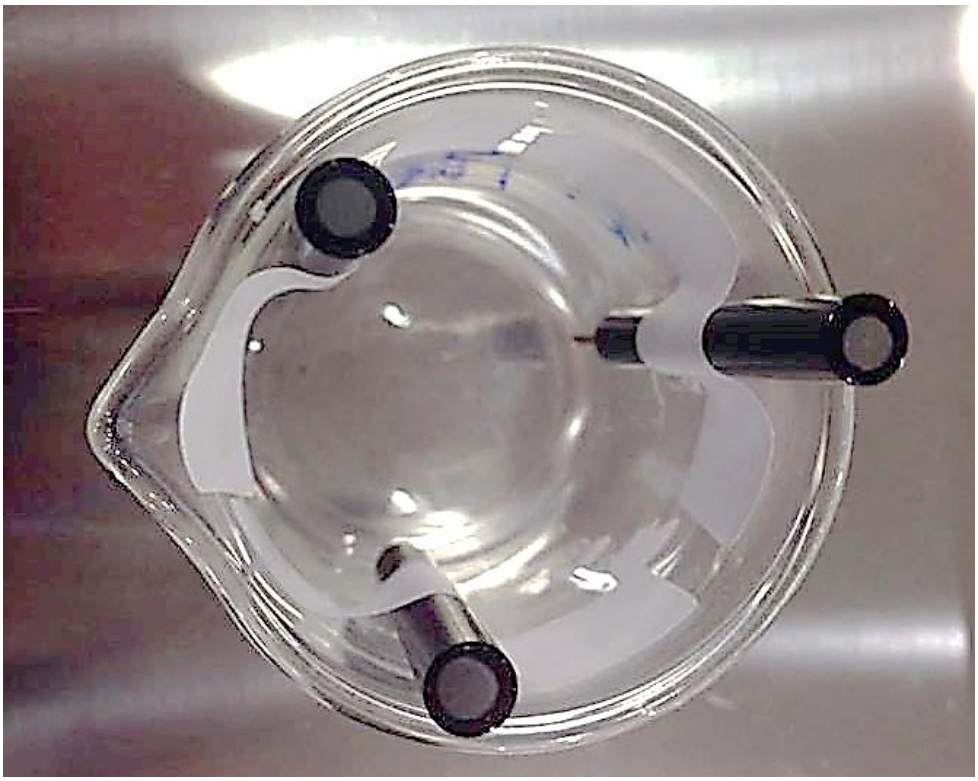

**Figure B.3 Dried at 50 °C, creating rGO film layer on the electrode sensor**

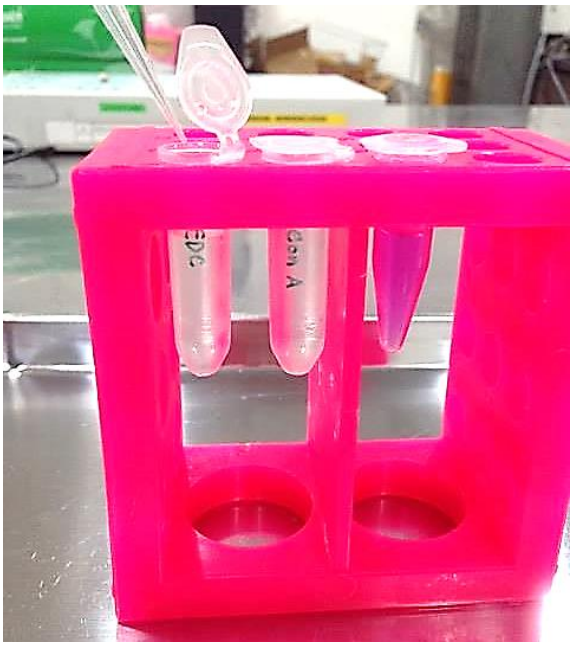


**Figure B.4 Droped 20 µl of EDC in MES buffer at pH 4.5 (10 mg/ml) after 2 hrs, droped 20 µl of Con A in PBS buffer with containing 1 mM $CaCl_2$ and $MnCl_2$ (3.82 mg/ml) for 30 mins, and then incubated with 20 µl of desired ovarian cancer cells for 30 mins**

**Figure B.5 Gently rinsed with PBS solution (pH 7.4)**

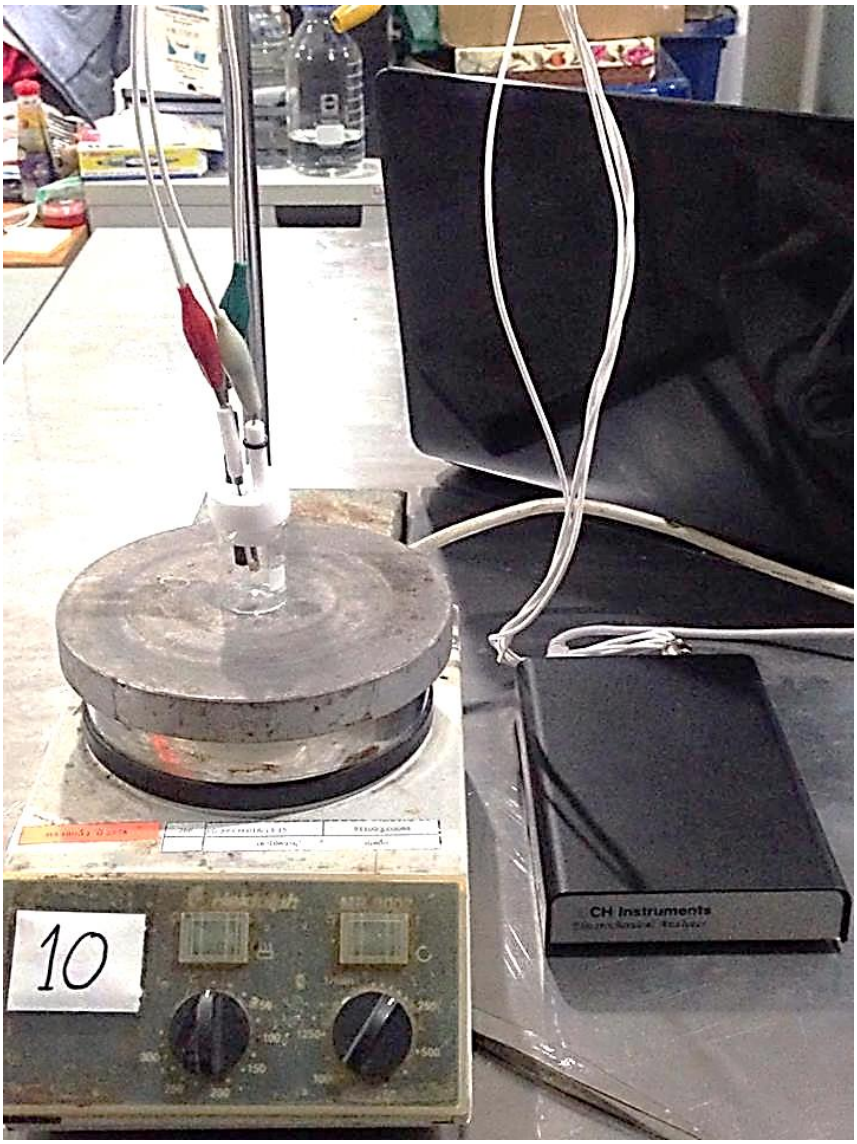


**Figure B.6 Electrochemical current was monitored and recorded as corresponded to the cyclic voltametry analysis**

# APPENDIX C

## Microscopy images of the ovarian cancer and fibroblast cells

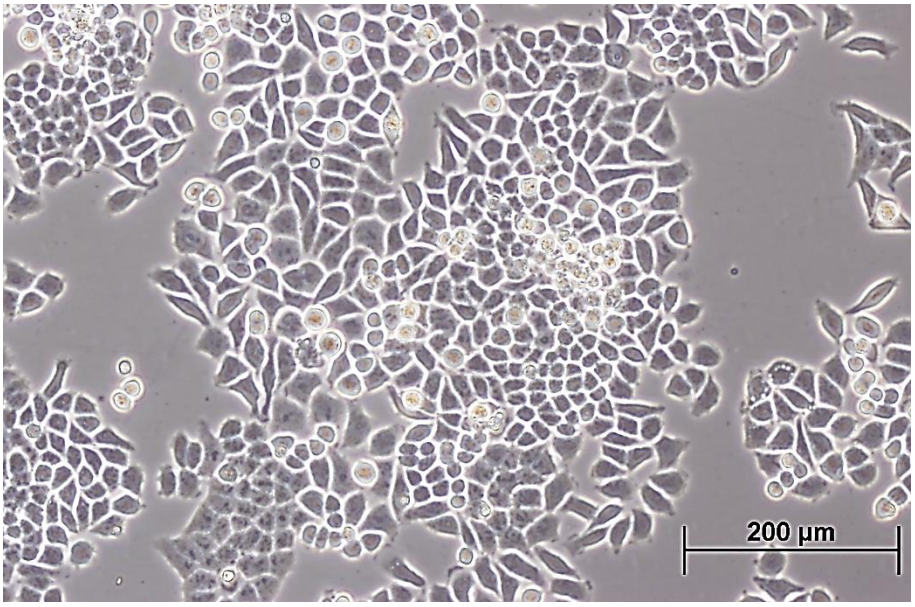


**Figure C.1 Image of ovarian cancer cells (A2780) at 10x magnification**

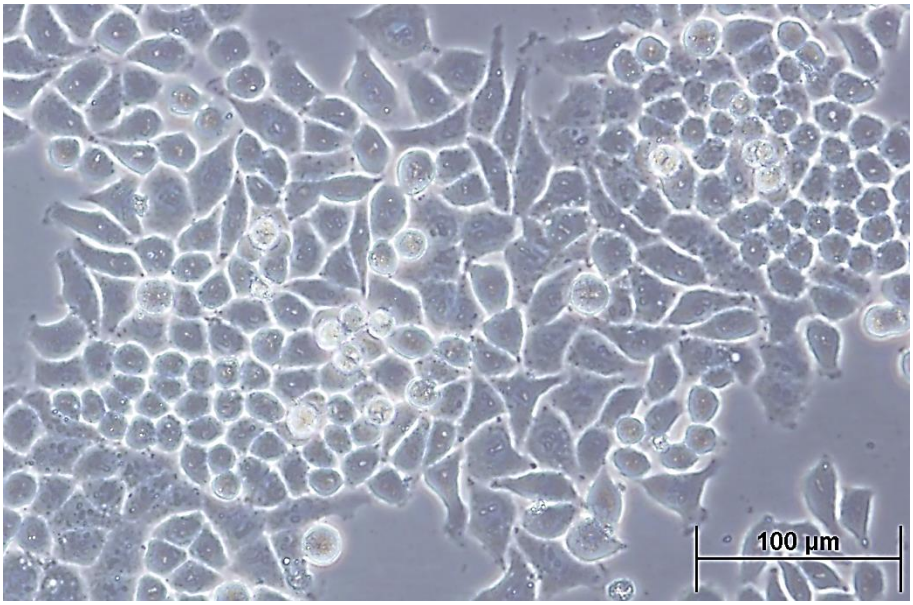


**Figure C.2 Image of ovarian cancer cells (A2780) at 20x magnification**


**Figure C.3 Image of fibroblast cells (L929) at 10x magnification**

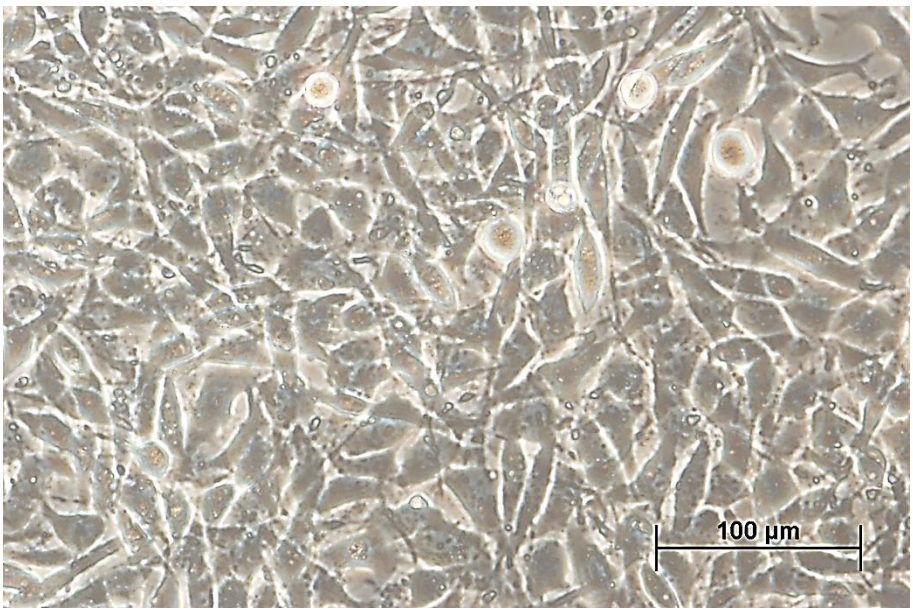


**Figure C.4 Image of fibroblast cells (L929) at 20x magnification**

# BIOGRAPHY


| | |
|---|---|
| **NAME** | Miss Chayanit Phatoomvijitwong |
| **DATE OF BIRTH** | 9 September 1992 |
| **PLACE OF BIRTH** | Bangkok, Thailand |
| **INSTITUTIONS ATTENDED** | Mahidol University, (2012-2015)<br>Bachelor of Chemical Engineering<br>Mahidol University, (2015-2017)<br>Master of Integrated Chemical Engineering |
| | The author would like to thank the financial support from the annual government grant under Mahidol University. |
| **HOME ADDRESS** | 5/83 Vararom village, Bangnon 5 Road,<br>Bangbon, Bangkok, 10150<br>Tel. 085-1463208<br>E-mail: chayanit.pha@student.mahidol.edu |
| **EMPLOYMENT ADDRESS** | Dept. of chemical engineering, faculty of engineering, mahidol university<br>25/25 puttamonthon 4Rd.<br>Nakornpathom, 73170 |